Sphingosine-1-Phosphate and Stromal Cells Contribute to an Aggressive Phenotype of Ovarian Cancer

Jack Guinan

Thesis submitted to the faculty of Virginia Polytechnic Institute and State University in partial fulfillment of the requirements for the degree of

Master of Science

In

Human Nutrition, Foods and Exercise

Eva M. Schmelz, Chair

Robert W. Grange

Irving C. Allen

May 19, 2017

Keywords: Ovarian cancer, sphingosine-1-phosphate, hypoxia, spheroids, stromal vascular fraction, sphingosine kinase 1

Abstract

Metastasis remains the largest contributor for ovarian cancer mortality. The five-year survival rate decreases dramatically as the disease advances from the primary tumor site to other organ sites within the peritoneal cavity. Thus, characterizing the mechanisms behind this metastatic potential may better elucidate the molecular mechanisms of ovarian cancer progression and may reveal novel targets for preventative and therapeutic treatments. Sphingosine-1-phosphate (S1P) is a critical secondary messenger responsible for many pro-cancer signals, e.g., proliferation, angiogenesis, inflammation, anti-apoptosis, and others. While S1P's role in the aggressive profile of many other cancers is well defined, its function in ovarian cancer development is less understood. The concentration of S1P is significantly increased in the ascites of women with malignant ovarian cancer, suggesting a role in ovarian cancer progression. This study aims to understand the importance of S1P in ovarian cancer metastasis. Using our well-characterized murine cell model for progressive ovarian cancer, we investigate the impact of S1P on ovarian cells and their interactions with the stromal vascular fraction recruited from the adipose tissue in culture conditions that mimic the physiologic environment of the peritoneal cavity. These studies will provide a mechanistic link of obesity, inflammation, and the increased risk of obese women to develop and die from ovarian cancer and identify signaling events as targets for interventions.

General Audience Abstract

The mortality rate of women diagnosed with ovarian cancer increases significantly as the disease metastasizes to other regions. Understanding the progression of this disease can create better detection and treatment methods, improving the outcome of women diagnosed with ovarian cancer. Sphingosine-1-phosphate (S1P) is a lipid molecule that has been implicated in many pro-tumorigenic properties in cancer cells; however, its role in ovarian cancer is less known. Stromal cells excrete high levels of S1P and are recruited into tumors for support and many other functions. Elucidating the role stromal cell incorporation into tumors and the role of S1P in ovarian cancer aggressiveness may highlight key pathways that can be targeted for screening methods and therapeutic treatments. This paper aims to understand the connections between S1P, stromal cells, and ovarian cancer as it progresses from a primary site to a metastatic, highly aggressive disease.

Acknowledgements

Dr. Schmelz—I do not know where to begin. You have been an invaluable part of my M.S. experience—both in curriculum and in research—as a mentor, professor, counselor, and friend. Your patience for my never-ending questions and curiosities about every little detail of my project is unrivaled; I would not be where I am today as a scientist without your knowledge and experience to guide me. While I am excited to begin this new chapter in my life, I cannot say that it will be easy to lose you as my mentor. Thank you so much for giving me this experience.

To Emily, Lu, and Alex, I cannot thank you enough for your help over the past two years. You all played such an important role in molding me into a research scientist and none of this would have been possible without you. To Kaley and Kelly, I am so grateful to have you as undergraduate research assistants. You have both played such an important role in assisting me with my research and this project could not have happened without you two.

Finally, I am incredibly grateful to my parents who have supported every choice I have made and always believed in me. Needless to say, I love you so much and I am so immensely lucky to have both of you in my life.

Table of Contents

List of Abbreviations

MOSE: Mouse ovarian surface epithelial cell line
- MOSE-E: Early stage
- MOSE-L: Late stage
- MOSE-L_{TICv}: Late stage, tumor initiating cell variant

S1P (Sphingosine-1-Phosphate): Bioactive first and second messenger sphingolipid.

BSA (Bovine Serum Albumin): Protein solution used to dissolve S1P.

SphK1 (Sphingosine Kinase 1): Membrane kinase that phosphorylates sphingosine into sphingosine-1-phosphate.

EMT/MET (Epithelial-mesenchymal transition or mesenchymal-epithelial transition): Proposed mechanism by which ovarian cancer cells can form into spheroids from a surface (EMT) and subsequently metastasize as a spheroid and adhere to another surface (MET).

MTT (3-(4,5-Dimethylthiazol-2-yl)-2,5-Diphenyltetrazolium Bromide): Dye metabolized by live cells to its formazan form that can measure cell viability via absorbance.

SVF (Stromal Vascular Fraction): Population of cells in adipose tissue that are not adipocytes.

HFD: High-fat diet.

DMEM (Dulbecco's Modified Eagle Medium)
- CS medium: DMEM +1% charcoal-stripped FBS
- LG medium: DMEM + 2 mM Glucose

Control medium: DMEM-HG (Dulbecco's Modified Eagle Medium – high glucose) + 5% FBS

List of Figures

List of Tables

I. Introduction

Ovarian cancer is the ninth most common type of cancer among women in the United States; however, it is the fifth leading contributor to death from cancer and the leading cause of death among gynecological cancers.[1] In 2016, an estimated 22,280 new cases of ovarian cancer will be diagnosed and an estimated 14,240 women will die of ovarian cancer.[2] The five-year survival rate decreases dramatically as the disease advances from the primary tumor site to other organ sites within the peritoneal cavity, from 92.1% when it is localized to the ovary to 28.8% when it has metastasized.[2] Lack of efficient detection methods in early stages of the disease lead to 60% of diagnoses after the disease has already metastasized and only 15% of diagnoses while the cancer is still confined to the primary site.[2] Understanding the mechanisms how ovarian cancer metastasizes and contributes to a significantly more lethal disease state is critical in developing better methods to detect this cancer and treatments to ameliorate or cure the condition. Ovarian cancer metastasis is a result of complex interactions within the peritoneal cavity including, but not limited to: anchorage-independent survival, aggregation into 3D tumor spheres, recruitment of stromal cells, and adaptation to a hypoxic, nutrient-deprived environment that contains high concentrations of sphingosine-1-phopshate. This study aims to elucidate the contributions of sphingosine-1-phosphate and stromal cells derived from adipose tissue to an aggressive, metastatic disease state of ovarian cancer. Understanding these interactions may reveal novel ways to assess the risk of ovarian cancer development and progression and may, furthermore, introduce pathways to target this disease for treatment.

II. Review of Literature

MOSE Cell Line

Our well-characterized mouse ovarian surface epithelial (MOSE) cell line mimics the progression of high-grade serous epithelial ovarian cancer from its benign state, MOSE-E (early stage) to a malignant state that induces ovarian carcinogenesis and tumorigenesis, MOSE-L (late stage) and, finally, to a highly aggressive, more efficient tumor-forming cell type, MOSE-L^{TIC_v} (late stage, tumor-initiating cell variant). This cell model utilizes normal MOSE cells that exhibit neoplastic transformation during *in vitro* culturing to represent these different stages of ovarian cancer development.[3] MOSE-E cells are an early, pre-malignant state that have a slow growth rate, an inability to undergo anchorage-independent growth, and cannot induce tumors in mice; they serve as a model for preneoplastic ovarian cancer.[3] MOSE-L cells exhibit rapid growth *in vitro*, an improved ability to have anchorage-independent growth, and have high tumorigenic potential in mice.[3] MOSE-L^{TIC_v} were generated by extracting tumor cells from the ascites in mice that were injected with the tumorigenic MOSE-L cells. MOSE-L^{TIC_v} are significantly more aggressive than MOSE-L cells, inducing a lethal disease in mice 23 days after injection of 10,000 MOSE-L^{TIC_v} cells, compared to 1,000,000 to 5,000,000 MOSE-L cells required to induce a similar lethal disease state in 8-10 weeks. MOSE-L^{TIC_v} cells thus mimic highly aggressive, fast-developing ovarian cancer. Figure 1 highlights some of the aggressive, metastatic phenotypes of MOSE-E to MOSE-L cells for comparison.

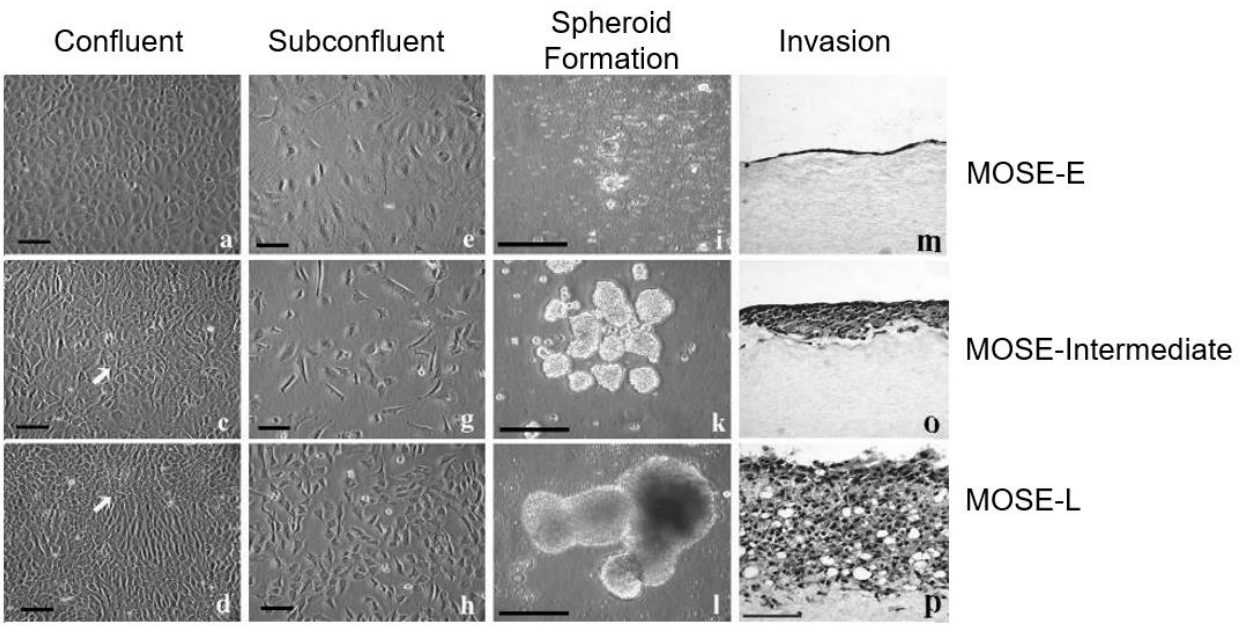

Figure 1. MOSE-E and MOSE-L cells with markers of aggressiveness. MOSE cell line progression, showing a decreased cell size, increased spheroid formation capacity, and an ability to invade in collagen in later stages.

Sphingosine-1-Phosphate

Sphingosine-1-phosphate (S1P) is a bioactive lipid first and second messenger implicated in several critical biological functions, including regulation of cell survival, angiogenesis, wound healing, cardiovascular function, immunity, neurogenesis, and others.[4, 5] Biosynthesis of S1P involves the reversible, ATP-dependent phosphorylation of a sphingosine molecule by a sphingosine kinase—SphK1 or SphK2.[6] A SphK1- and SphK2-knockout in mice induces embryonic lethality, highlighting the importance of this signaling molecule in several key developmental and regulatory mechanisms.[5] *De novo* synthesis of S1P (Fig. 2) begins with the condensation of serine and palmitoyl CoA by serine palmitoyltransferase in the endoplasmic reticulum to yield 3-ketodihydrosphingosine.[7] Through a series of reactions and sphingolipid intermediates, 3-ketodihydrosphingosine is converted to ceramide, which is then transported in a non-vesicular manner to the Golgi apparatus by ceramide transfer protein (CERT).[8] In the Golgi

apparatus, ceramide acts as a substrate for the synthesis of several complex sphingolipids, such as sphingomyelin (SM) and other glycosphingolipids.[7] Complex sphingolipids—such as SM—are thought to be transported in a vesicular manner from the Golgi to the plasma membrane.[9] The plasma membrane holds the highest concentration of cellular SM, which is a key mediator in synthesis of other sphingolipids.[10] SM ⇋ ceramide conversion is regulated by several enzymes in the plasma membrane, secretory sphingomyelinase and sphingomyelin synthase 2 in the outer leaflet and neutral sphingomyelinase in the inner leaflet.[10] Ceramide is then metabolized by ceramidase to yield sphingosine, which is then subsequently phosphorylated by sphingosine kinase 1 (SphK1) in the plasma membrane.[7]

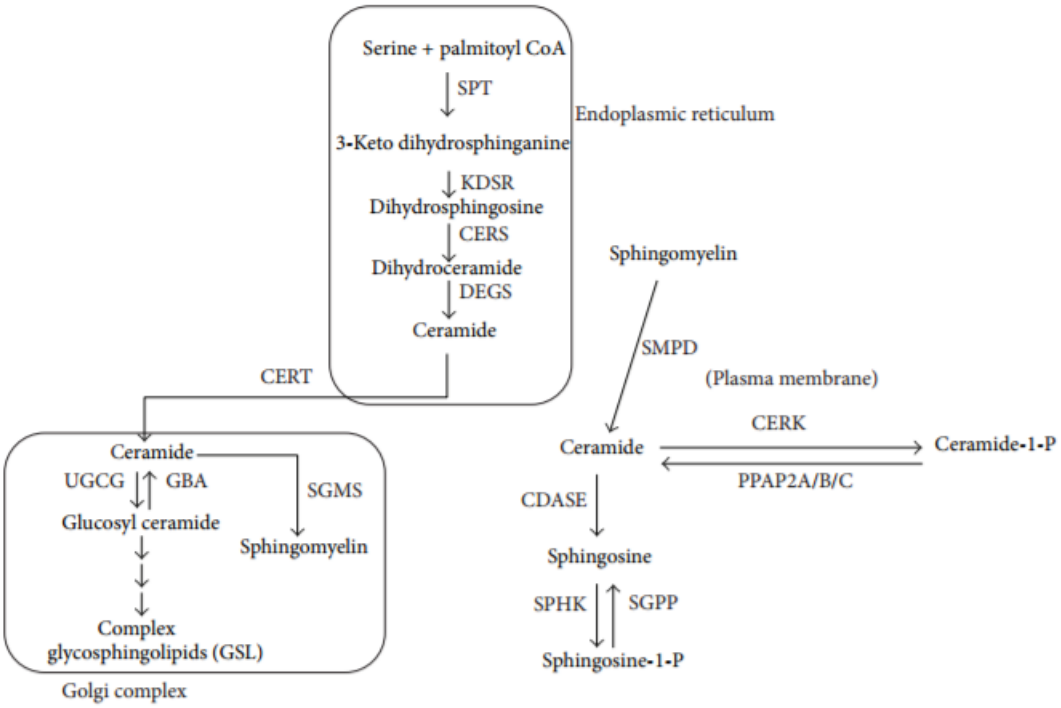

Figure 2. *De novo* synthesis of sphingolipids. Synthesis of sphingosine-1-phosphate occurs when sphingomyelin is exported from the Golgi complex to the plasma membrane and is metabolized by enzymes in lipid rafts to yield sphingosine, which is then phosphorylated by sphingosine kinase 1. Image taken from Rao et al.[7]

Ceramide acts partly as a counterpart to S1P in its ability to induce apoptosis in cells; moreover, it plays a critical role in immune and inflammatory responses, and serves as a regulator

of protein secretion.[11] Normal levels of ceramide and S1P are tightly regulated by cells to ensure a balance of their inherently opposite effects in cells—particularly in apoptosis/survival. It was established in the beginning of the sphingolipid research field that the balance of intracellular levels of ceramide and S1P is critical in deciding cell fate.[12] Thus, regulation of these two molecules is key in maintaining cellular homeostasis. An imbalance of this sphingolipid rheostat is key in cancer cell development and tumorigenesis. In cancer cells, an upregulation of S1P facilitates tumor progression and metastasis via promotion of cancer cell survival, angiogenesis, migration, immune response, and other pro-metastatic functions (Fig. 3).[13, 14] Elevated S1P concentrations in cancer cells correlate with a significant upregulation in SphK1 expression[14] and its role in promoting aggressive cancer development is well-established in many cancers; however, its role in ovarian cancer progression is less understood. S1P concentrations have been shown to be significantly upregulated in the ascites of women diagnosed with malignant ovarian cancer;[15-18] potentially secreted by platelets,[19] the cancer cells themselves, or other cell types. Furthermore, it has been shown that SphK1 is highly upregulated in the tumor stroma of high-grade serous ovarian cancer.[20] Ceramide, on the other hand, acts as a critical tumor suppressor in its ability to induce apoptosis, block cell cycle transition, and commence autophagic responses in cancer cells.[21]

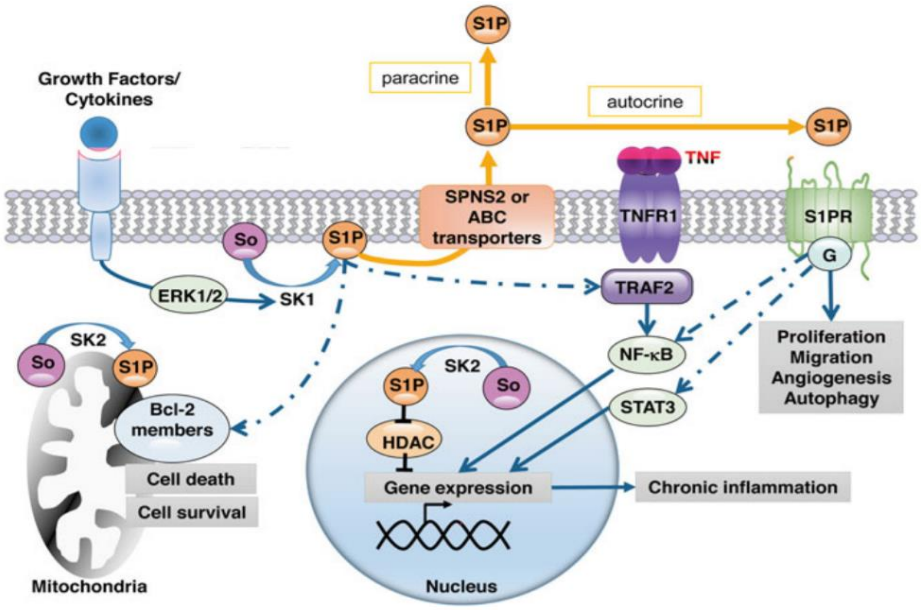

Fig 3. Generic S1P pathways. Stimulation of S1P production from a growth factor/cytokine to act as a first messenger (binding to $S1PR_{1-5}$) or second messenger (acting on pathways within the cell after release). Image from Hannun et al.[22]

S1P can act as a first or second messenger upon activation by a growth factor (Fig. 3) and bind to any of its five receptors ($S1PR_{1-5}$).[22] The cascades of S1P binding to its receptors are inherently complex; they are cell-specific and depend on which receptor S1P binds to.[23] In general, S1P can induce motility and promote survival in cancer cells via $S1PR_1$ or $S1PR_3$, while it can inhibit cancer cell motility through via $S1PR_2$ (Fig. 4).[23] After binding to these specific S1P receptors that are expressed on cancer and stromal cells, S1P can activate signaling pathways that enhance adhesion, motility and invasion, implying a critical role in the cancer cells' metastatic and deadly potential.[14] Previous studies in our lab demonstrate the ability for S1P to induce a flatter phenotype in MOSE-E and MOSE-L cells, with some subpopulations demonstrating increased actin bundling (Fig 5).[24] Furthermore, S1P increased the membrane capacitance (a measurement for the integrity of biological membranes that includes surface topography, resistance and membrane potential) and surface ruffles in MOSE cells towards a more tumorigenic phenotype cells while sphingosine lowered both membrane capacitance and surface ruffles towards the

properties of benign cells.[25] This suggests S1P may contribute to a malignant phenotype in ovarian cancer cells.

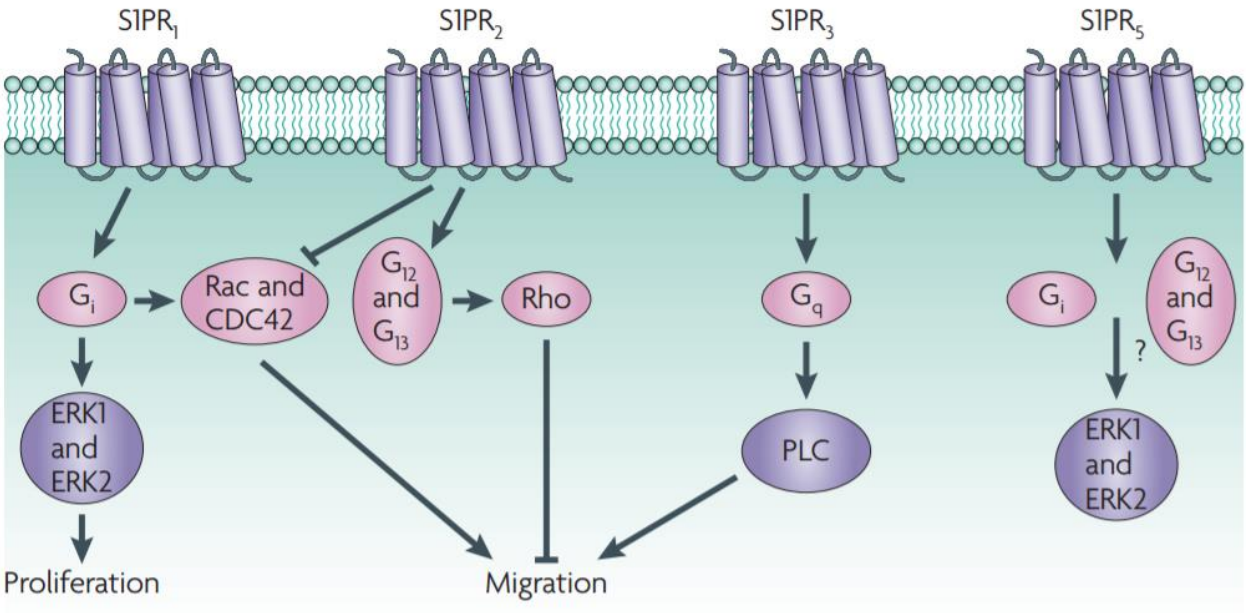

Fig 4. Example pathways/effects of S1P upon binding to $S1PR_{1\text{-}3,5}$. Image from Pyne and Pyne.[23]

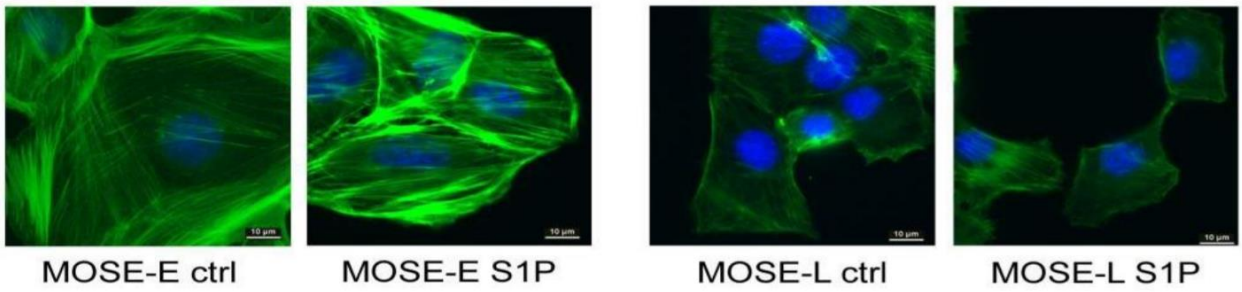

Fig 5. Actin and phalloidin staining of MOSE-E and MOSE-L cells after 8 hour treatment with 500 nM S1P. Image from Creekmoore et al.[24]

Sphingolipids thus play a critical role not only in regulating normal cell development, growth, and maintenance, but also in modulating cancer cell proliferation, migration, invasion, and metastasis. S1P is well known for its pro-tumorigenic properties; however, it is not well known if these mechanisms are attributed to high intracellular S1P from upregulated endogenous SphK1, or binding of S1P from supporting cells recruited by the cancer cells. Many interactions

of S1P in cancer remain to be elucidated—e.g. role of different S1PRs, interactions with other sphingolipid metabolites, the impact of a hypoxic environment, and the heterogeneous nature of tumors.

Epithelial Ovarian Cancer Development and Spheroid Formation

Ovarian cancer development and progression stems from a series of complex interactions including an altered differentiation pattern in epithelial cells, epithelial-mesenchymal transition (EMT), spheroid formation in the peritoneal cavity, recruitment of tumor-associated cells, and local and distant metastasis, perhaps via mesenchymal-epithelial transition (MET). EMT is the proposed mechanism by which epithelial ovarian cancer cells acquire the ability to metastasize into the peritoneal cavity.[26] EMT is strongly correlated with a loss of E-cadherin expression in ovarian epithelial cells and subsequent development of an aggressive, metastatic phenotype—including spheroid generation.[26] Spheroids are compact, 3D cellular structures that have distinct characteristics from their monolayer counterparts, including a slower doubling rate, increased resistance to chemotherapeutic drugs, increased stem-like properties, and an efficient metabolic adaptation to a hypoxic tumor environment.[27] Normal median oxygen varies from 3.4-6.8% across all tissues, whereas median oxygen levels in all tumor types ranges from 0.3-4.2%.[28] Furthermore, analysis of ascites developed from bacterial peritonitis indicate that ascites host a nutrient-deprived environment, with glucose levels ranging from 4.3 to 8.7 mM.[29] Successful transition into the peritoneal cavity and subsequent successful tumor formation thus requires spheroids that can adapt to a hypoxic, nutrient-deprived environment. Spheroids extracted from the ascites of patients with stage III or IV ovarian carcinoma have shown some ability to adhere on certain matrices and invade other cellular monolayers.[30] The EMT model of cancer metastasis (Fig. 6) highlights the progression of malignant ovarian cancer cells to a metastatic phenotype via EMT and increased

stemness to form complex 3D spheroids that adapt to the nutrient-deprived environment of the peritoneal cavity for efficient local and subsequent distant metastasis with their ability to re-adhere to surfaces (perhaps due to MET) and invade other cellular monolayers. Successful tumor formation after metastasis requires these spheroids to adapt to an increasingly hypoxic environment.

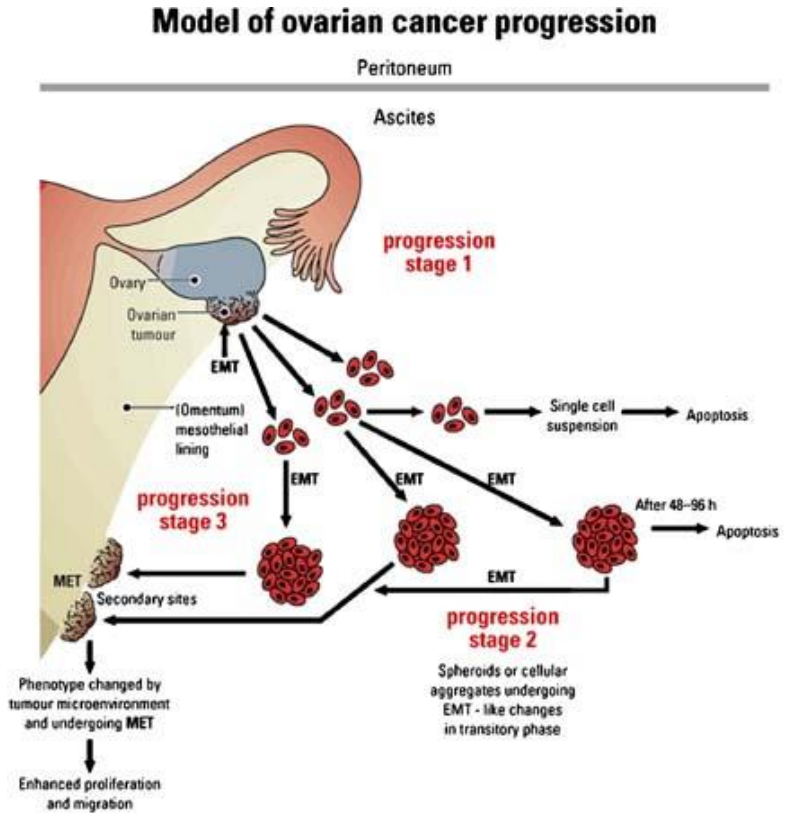

Fig 6. A model of ovarian cancer progression and metastasis via EMT transition. Image from Ahmed et al.[26]

Tumor Microenvironment

Tumors are complex structures that include not only cancer cells, but other recruited cells to promote survival of the tumor via angiogenesis, immunoprotection, and energy support. In general, cells in the tumor microenvironments can be divided into three categories: (1) cells of

hematopoietic origin, such as T cells, B cells, macrophages, neutrophils, and natural killer cells; (2) cells of mesenchymal origin, such as fibroblasts and adipocytes, and cancer and other epithelial stem cells; (3) non-cellular components, i.e. the extracellular matrices (ECMs).[31] Macrophages are well documented in their ability to upregulate certain hypoxic transcription factors (VEGF, HGF, MMP2, IL-8) upon recruitment by a tumor.[32] Neutrophils are implicated in their angiogeneic potential upon tumor incorporation.[32] Other immune cells are less understood in their pro-tumorigenic properties, and their function—immunosuppression, other angiogeneic functions—varies across different types of tumors.[32] Cancer-associated fibroblasts have been implicated in several tumor-protective and tumor-proliferative roles, including the exportation of growth factors for tumor support, synthesis of chemokines for other cell recruitment, and promotion of an invasive phenotype.[33] The altered ECM in a tumor microenvironment plays a similarly critical role as the tumor-associated stromal cells. Alteration of the ECM via tumor development promotes an inflammatory environment, an upregulation of angiogenesis, and increased motility and metastatic potential of the tumor cells and tumor-associated cells.[34] The tumor microenvironment (Fig. 7) is thus an intricate association of a diverse cell population and an altered ECM that promote tumor development and sustainment, rendering treatment of tumors (i.e. via chemotherapeutic agents) incredibly complicated due to its heterogenetic nature.

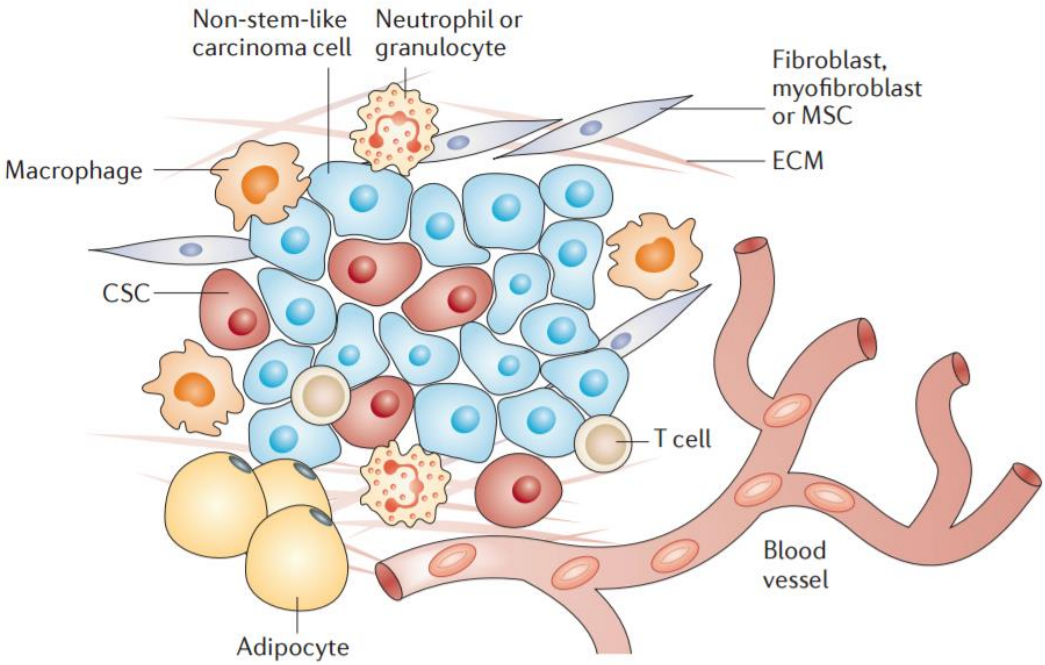

Fig 7. Illustration of the heterogeneous tumor microenvironment with recruited cells. Image from Pattabiraman and Weinberg.[31]

Tumor microenvironments vary among cancer types (perhaps due to environmental and/or tumor progression differences, among others); thus, the ovarian tumor microenvironment is a distinct construct that contains cancer cells but also fibroblasts, mesenchymal stem cells, macrophages, and other peritoneal cell.s.[35] These cells are also found in the stromal vascular fraction of white adipose tissue[36, 37] and can be recruited to the tumor—or perhaps earlier, in the peritoneal cavity to disseminating cancer spheroids—where they aid in many of its malignant functions such as proliferation and chemoresistance.[35] Our lab has previously shown the association between MOSE cells and the stromal vascular fraction (SVF) of the parametrial white adipose tissue (WAT) of female C57BL/6 mice on a high fat diet (Fig. 8).[38] Stromal cells were incorporated into the core of the MOSE-L_{TICv} spheroids when co-cultured simultaneously (A and B) or when stromal cells were added 24 hours after MOSE-L_{TICv} cells were seeded (C and D).

Furthermore, we have previously shown that the SVF cells MOSE-L_{TICv} cells in heterogeneous spheroids increase the invasive capacity of the spheroids and invade jointly in collagen (Fig. 9).[38] These results indicate that ovarian cancer cells recruit stromal cells in spontaneous spheroid formation and that the stromal cells are recruited in the invasive structures of the cancer cells. Investigating the role of the stromal cells in ovarian cancer development and progression is critical in elucidating the mechanisms behind which ovarian cancer successfully metastasizes and develops into a potentially lethal disease. While several studies have highlighted the importance of certain recruited cells into the tumor microenvironment, much remains to be investigated about their exact function in ovarian cancer progression.

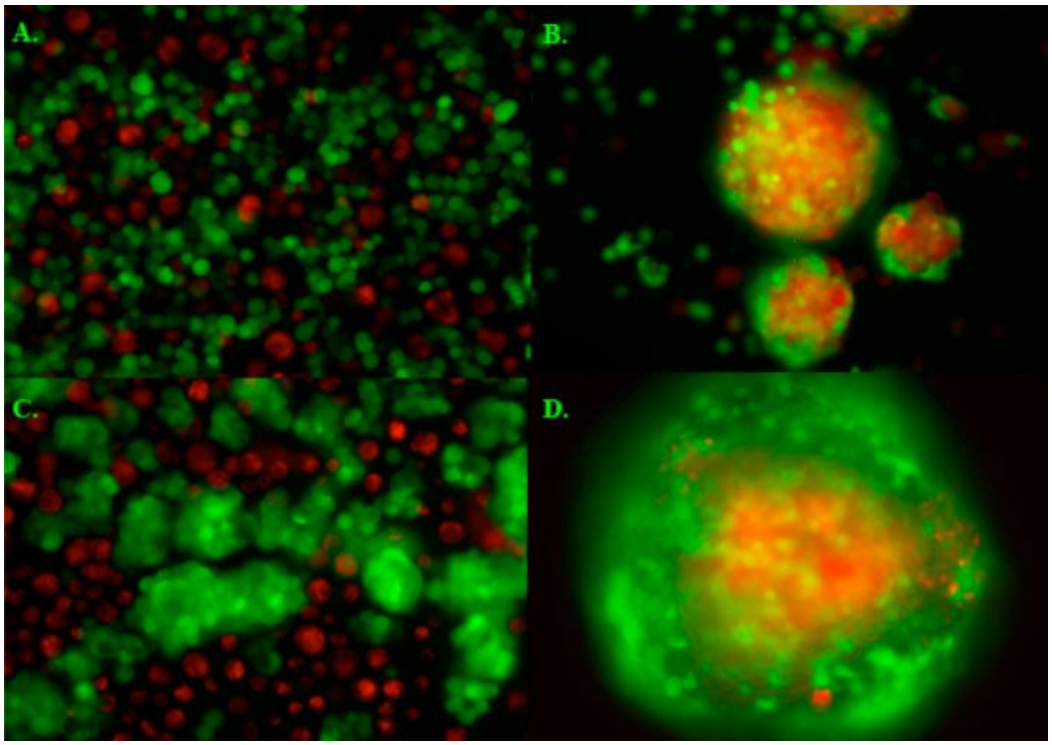

Fig 8. Association of MOSE cells and SVF cells. Heterogeneous spheroid formation of MOSE-L_{TICv} (green) and SVF (red) when co-cultured simultaneously (A and B) or when SVF cells were added 24 hr after MOSE-L_{TICv} seeding. Image from Shea.[38]

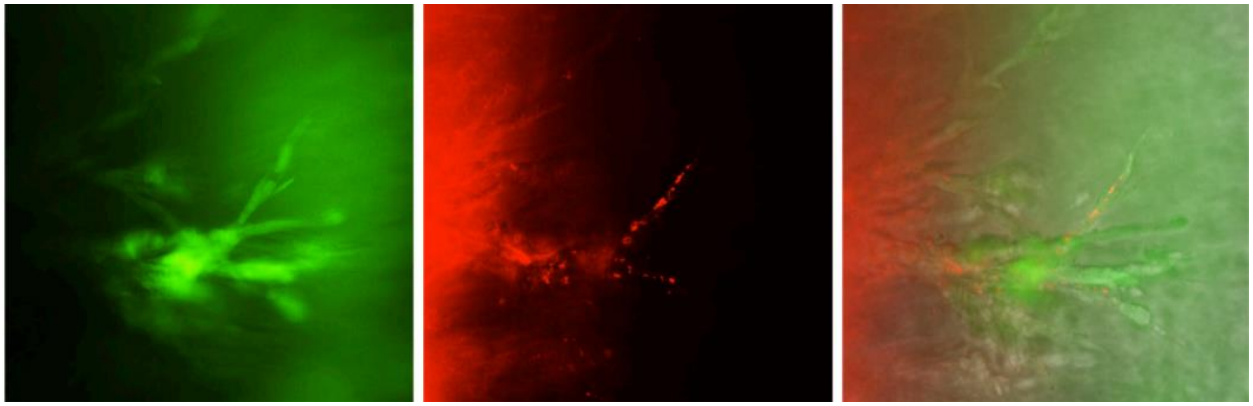

Fig 9. Invasion of a heterogeneous MOSE-L_{TICv} (green) and SVF (red) spheroid in collagen. Image from Shea.[38]

Obesity

An overweight or obese BMI has been implicated as a significant risk factor for a variety of cancers, including endometrial cancer, esophageal adenocarcinoma, gastric cardia cancer, liver cancer, kidney cancer, multiple myeloma, meningioma, pancreatic cancer, colorectal cancer, gallbladder cancer, and breast cancer.[39] However, high abdominal body fat deposit—not necessarily BMI—contributes to the risk of ovarian cancer development,[40] due to the pro-inflammatory environment, and the accessibility of energy (lipolysis induced by cancer cells).[41] While the exact mechanisms behind which a high abdominal fat deposit contributes to an aggressive phenotype of ovarian cancer remains to be elucidated, previous studies in our lab have shown that the number of white adipose tissue-derived cells is significantly increased in the parametrial fat of mice fed a high-fat diet.[38] This may indicate that an increased number of recruited stromal cells—in addition to an inflammatory environment—may result in a more aggressive disease state.

Conclusion

The multifaceted and complicated nature of ovarian cancer progression and heterogeneous tumor development yields a complicated approach to therapeutic treatments—particularly due to the lack of early detection methods before the disease metastasizes into a more lethal condition. Understanding the mechanisms that contribute to an aggressive ovarian cancer phenotype could reveal novel targets for treatments that might involve targeting certain pathways—S1P—or cell types—stromal cells—rather than the tumor cells themselves. To understand the mechanisms underlying ovarian cancer's metastasis and the importance of high central body fat in its development, the interactions between recruited stromal cells and the cancer cells must be elucidated in culture conditions that mimic those in the malignant ascites. Specifically, we will investigate the response of cancer cells to S1P in 3D culture conditions with very low-glucose (2 mM) levels and/or low-nutrient conditions (1% charcoal-stripped FBS) in a hypoxic environment (1.0%) to mimic conditions that ovarian cancer cells must adapt to for successful metastasis.[42] To examine if S1P secretion by stromal cells is critical in ovarian cancer progression, these conditions will be mimicked with the incorporation of SVF cells from the parametrial fat from mice fed a high-fat (60% kcal from fat) diet without S1P supplementation. This study aims to understand the mechanisms underlying the protective and proliferative signals of S1P potentially excreted from recruited stromal cells on cancer cells as the disease progresses from an early stage (adherent cancer cells) to metastasis.

Specific Aims

The experiments utilized in this paper highlight the impact of S1P or SVF cells in their ability to influence cell viability, spheroid size, spheroid outgrowth, and spheroid invasion in collagen of MOSE cells. This approach mimics the progression of the disease from an adherent monolayer (cell proliferation) to its exfoliation and formation of spheroids in the peritoneal cavity (spheroid size) to its subsequent adhesion to other surfaces within the peritoneal cavity (spheroid outgrowth) and finally its invasion into extracellular matrices and other tissue (spheroid invasion in collagen). This paper aims to highlight where in the metastatic profile S1P and/or SVF cells contribute to ovarian cancer progression by comparing these treatment groups—to elucidate whether any upregulation of aggressive phenotype markers is due to S1P itself or via other mechanisms contributed from the stromal cells.

SA 1: Determine the impact of sphingosine-1-phosphate on ovarian cells representing progressive ovarian cancer.

Working Hypothesis: In a concentration-dependent manner, S1P will affect cell viability and invasive potential of MOSE cells as a function of disease stage and culture conditions.

Rationale: Exfoliated ovarian cancer cells encounter malignant ascites containing low concentrations of glucose, a low-oxygen environment but high concentrations of S1P.

Experimental Plan: MOSE cells of varying aggressiveness (MOSE-E → MOSE-L → MOSE-L_{TICv}) will be treated with S1P in both adherent and 3D conditions, in normoxia and hypoxia.

We will evaluate:

a. Cell proliferation
b. Spheroid growth & viability in relevant culture conditions
c. Outgrowth and invasion changes with S1P treatment

SA 2: Determine the changes in the proliferative and invasive potential of MOSE spheroids when co-cultured with SVF from adipose tissue.

Working hypothesis: SVF from adipose tissue will enhance the aggressive phenotype of MOSE spheroids as a function of disease stage and culture conditions.

Rationale: Stromal cells derived from white adipose tissue play a critical role in tumor proliferation and survival. Ovarian cancer risk is increased with high central body fat.

Experimental plan: We will isolate the stromal vascular fraction from the visceral tissue of mice fed a high-fat diet and co-culture these cells with MOSE cells, increasing aggressive phenotype in 3D conditions. To mimic peritoneal conditions, we will also expose the cells to hypoxia and nutrient deprivation and evaluate the response to S1P treatment.

We will evaluate:

a. Spheroid growth & viability
b. Effectiveness of SVF cells and S1P in rescuing spheroids in nutrient-starved conditions
c. Outgrowth and invasion modulations in starved conditions from co-culturing with SVF cells

SA 3: Evaluate the effectiveness of a SphK1 inhibitor on controlling cell proliferation

Working Hypothesis: Treatment of the SVF cells with the SphK1 inhibitor will decrease the proliferation of MOSE cells.

Rationale: SphK1 is upregulated in the tumor stromal cells, perhaps enhancing tumor proliferation and aggression.

Experimental Plan: Analyze cell viability against increasing concentrations of a SphK1 inhibitor (Webster Santos – Virginia Tech).

We will evaluate:

a. Cell Proliferation

III. MATERIALS AND METHODS

Normoxia

Normoxic conditions were maintained using atmospheric oxygen in a humidified incubator that upheld 5% CO_2 at 37°C.

Hypoxia

A hypoxic environment (1% O_2, 5% CO_2) was maintained using a humidified sealed chamber connected to a CO_2 and O_2 controller (BioSpherix) at 37°C.

Cell Culture Maintenance

MOSE cells and SVF cells were maintained in medium from powdered high glucose Dulbecco's Modified Eagle Medium [-sodium bicarbonate] (Sigma), supplemented with 5% fetal bovine serum (Atlanta Biologicals), 100 mg/mL penicillin and streptomycin (JR Scientific), and

3.7 g/L sodium bicarbonate (Fisher), set to a pH of 7.2. Medium was filter sterilized with 0.22 μm filters from Millipore.

Starved Medium Conditions

Nutrient-starved medium was made using medium from powdered Dulbecco's Modified Eagle Medium [-glucose, -sodium pyruvate, -glutamate, –phenol red, -sodium bicarbonate] (Sigma) supplemented with 3.7 g/L sodium bicarbonate, 0.11 g/L sodium pyruvate (Sigma), 0.584 g/L L-glutamine (Fisher) and 100 mg/mL penicillin and streptomycin (JR Scientific).

Low-glucose (2 mM) medium was created using the nutrient-starved medium supplemented with filter-sterilized glucose solution (Sigma) in PBS.

Charcoal-stripped fetal bovine serum (Atlanta Biologicals) was made using the nutrient-starved medium with 1% (v/v) charcoal-stripped fetal bovine serum.

Sphingosine-1-Phosphate Solution

S1P powder (Avanti Lipids) was dissolved in 60 μM BSA (in PBS) at 500 μM stock concentration stored in -20°C and used within three months of freezing.

S1P was dissolved using a methodology adapted from Avanti Lipids.[43] S1P powder was added to 95% methanol (in dH_2O) at 0.5 mg/mL concentration in a glass test tube. S1P was sonicated until a hazy, grey solution was formed. Methanol was evaporated using a dry stream of nitrogen. 60 μM BSA solution was added to a final 500 μM S1P stock concentration. The solution was sonicated until S1P was completely dissolved. Stock solutions were aliquoted and stored in -20°C.

Stromal Vascular Fraction (SVF) Isolation

Female C57BL/6N mice (Harlan Laboratories) were housed five per cage with ad libitum access to water and high-fat diet (60% kcal from fat [lard], Teklad Diets) under a 12-hour light/dark cycle environment at 21°C. The high-fat diet induced obesity and mice were sacrificed at 31 weeks of age (45 g average body weight) by CO_2 asphyxiation. All conducted animal procedures were approved by the Virginia Tech Institutional Animal Care and Usage Committee (IACUC).

SVF cells were isolated from visceral fat pads (primarily parametrial fat) from the peritoneal cavity given a standard protocol.[44] Extracted adipose tissue was rinsed in Krebs-Ringer bicarbonate buffer (118 mM NaCl, 5 mM KCl, 2.5 mM $CaCl_2$, 2 mM KH_2PO_4, 2 mM $MgSO_4$, 25 mM $NaHCO_3$, 5 mM glucose, pH set to 7.4), minced, and digested in a collagenase solution (1 mg type IV collagenase, 10 mg BSA, and 2 mM $CaCl_2$ in 1 ml PBS). Adipose tissue was digested in the collagenase solution for 1 hour in a 37°C water bath, with shaking every 5-10 minutes. Samples were then centrifuged at 300 *g* until the SVF was separated from adipocytes. The top layer (oil, primary adipocytes) were aspirated, with the SVF cells remaining on the bottom. SVF cells were washed in warm PBS (with 1% BSA) and subsequently centrifuged at 300 *g* again. The top layer was again aspirated to ensure purity of the SVF, completely separated from the adipocytes. Remaining SVF cells were plated in tissue-culture treated T75 flasks (Falcon) with high-glucose DMEM (Sigma) supplemented with 5% FBS (Atlanta Biologicals), 100 mg/mL penicillin and streptomycin (JR Scientific) and 1x ciprofloxacin (Genhunter). After 24 hours, medium was aspirated to remove dead cells and debris. Attached cells were washed with PBS and supplemented with fresh medium. After reaching 80% confluency, cells were trypsinized and cryogenically stored until usage. Upon thawing, SVF cells were counted and used immediately in spheroids to avoid differentiation of the SVF with further plate passaging.

MTT Assay

MTT assays were performed in three biological replicates for each cell line. MOSE-E cells were seeded at 2,000 cells/well, MOSE-L cells were seeded at 1,000 cells/well, and MOSE-L_{TICv} were seeded at 500 cells/well (100 μL in each well for each cell type) in 48-well tissue culture-treated plates (Corning). 2X treatment (S1P) was added 4 hours after seeding 100 μL).

MTT powder (Biosynth) (2 mg/mL) was dissolved in PBS, filter sterilized and stored for up to one month in 4°C. Lysis buffer was prepared (20 g SDS, 40 mL deionized water, 40 mL N,N-dimethylformamide, 2.5 mL 1N HCl, and 2.5 mL 80% acetic acid) and stored at room temperature.

Cells were grown for 72 hours. After 72 hours, 150 μL of MTT solution was added to each well and incubated at 37°C for 1.5 hours. Medium + MTT solution was aspirated and 200 μL of lysis buffer was added and left overnight. Absorbance was read with a platereader at 570 nm.

Spheroid Formation and Maintenance

Single spheroids were formed at a density of 2,000 cells per well in 96-well, ultra-low adherence plates (Corning) at a 100 μL volume in numerous samples of 3 biological replicates. After seeding, plates were centrifuged for 3 minutes at 900 RPM. Any treatment of spheroids was added 24 hours after centrifugation at a 100 μL volume (2X treatment) for a final volume of 200 μL with 1X treatment. 10-day spheroid experiments had 30 μL medium added at each Day 1, 5, 8, and 10 to ensure constant treatment and to compensate for evaporation. Co-cultured, heterogeneous spheroids were seeded at a 2,000 cell/well density with a 2:1 MOSE:SVF cell ratio.

Spheroid Size

Spheroid size was measured in three biological replicates for each cell line at days 1, 5, 8, and 10. The area of each spheroid at each time point was measured using NIS-Elements software.

Outgrowth Assay

Spheroids were seeded at a 2,000 cell/well density in 3 biological replicates with numerous samples. Spheroids were transferred from 96-well ultra-low adherence plates to 48-well tissue-culture treated plates (Corning) after 5 days of treatment. Pictures were taken of spheroid adhesion to the plate at 24 hours. Outgrowth area was measured by subtracting total cellular outgrowth from spheroid area.

Cell Tracker

Stromal cells were incubated with 1 μM FM-DiI (Molecular Probes) in D-PBS for 5 minutes at 37°C and then 15 minutes at 4°C. Cells were washed with D-PBS and then put back into medium for subsequent seeding.

Invasion Assay

Cells were seeded at a 10,000 cells/well density as either homogeneous or 2:1 cancer cell:SVF heterogeneous spheroid in a 96-well ultra-low adherence plate (Corning). Treatments (S1P, BSA) were added 24 hours after seeding. After 48 hours of treatment, medium from was removed to a final volume of 30 μL. All ingredients of the collagen assay were kept on ice. Per well composition: 30 μL spheroid and medium, 2.78 μL of 10X concentrations of DMEM (Sigma), 3.22 μL dH_2O, 0.75 μL of sterile 1N NaOH, and 21 μL of 5 mg/mL type I collagen from rat tail (Ibidi). 27.75 μL of the mixture was added to each well for a final collagen concentration of 1.75

mg/mL and the spheroid/collagen mixture was mixed using a pipette to ensure implantation within the collagen. Plates were placed in the incubator at 37°C for an hour to allow collagen to set. 50 μL of respective medium was added to each well. Pictures were taken after 24 hours.

SphK1 Inhibitor

SphK1 inhibitor was obtained from Dr. Webster Santos from the Chemistry Department at Virginia Tech. Stock solutions were dissolved in DMSO at 2 mM concentrations and stored at -20°C.

Statistics

Data is presented as mean ± SEM or percent control ± SEM. Results were analyzed with one-way or two-way ANOVA and considered significant at $p < 0.05$ (Microsoft Excel).

IV. RESULTS

S1P Enhances Cell Proliferation of Adherent Malignant MOSE Cells

MOSE-E, MOSE-L, and MOSE-L^{TICv} cells were incubated with increasing concentrations of S1P (0.5 μM to 10 μM) for 72 hours and subsequently analyzed by an MTT assay to assess the effect of S1P on cell proliferation under both normoxia and hypoxia. MTT is a substrate that is metabolized by cells to formazan that has a peak absorbance near 570 nm; absorption is strictly correlated to the number of viable cells.[45] MOSE-L and MOSE-L^{TICv} cells responded to the S1P under both conditions with an increase in proliferation up to a certain concentration (Figs. 10 and 11). Under normoxia, MOSE-L and MOSE-L^{TICv} had increased proliferation up to a concentration of 5 μM S1P and experienced toxicity at a 10 μM concentration (Fig 11). However, under hypoxia, MOSE-L cells had a more robust reaction to S1P and did not show toxic effects at 10 μM S1P,

whereas the MOSE-LTICv cells still experienced a decreased proliferation rate at a 10 μM concentration (Fig. 10). The benign MOSE-E cells did not respond positively to S1P at any concentration and were consequently excluded from further S1P and SVF analyses. These results indicate that malignant MOSE cells respond to S1P treatment with enhanced proliferation; however, MOSE-E cells did not react to S1P at any concentration since proliferation is a key part of early cancer progression. Thus, S1P in concentrations that can be found in malignant ascites is not implicated in preneoplastic, monolayer cell proliferation but supports the growth of MOSE-L cells representing slow-developing disease. 1 μM S1P treatment was chosen as the standard for the rest of the experiments for better comparison to previous studies in our lab and to avoid inundation of cells with S1P at higher concentrations. Furthermore, this is a concentration that can be found in malignant ascites.[15]

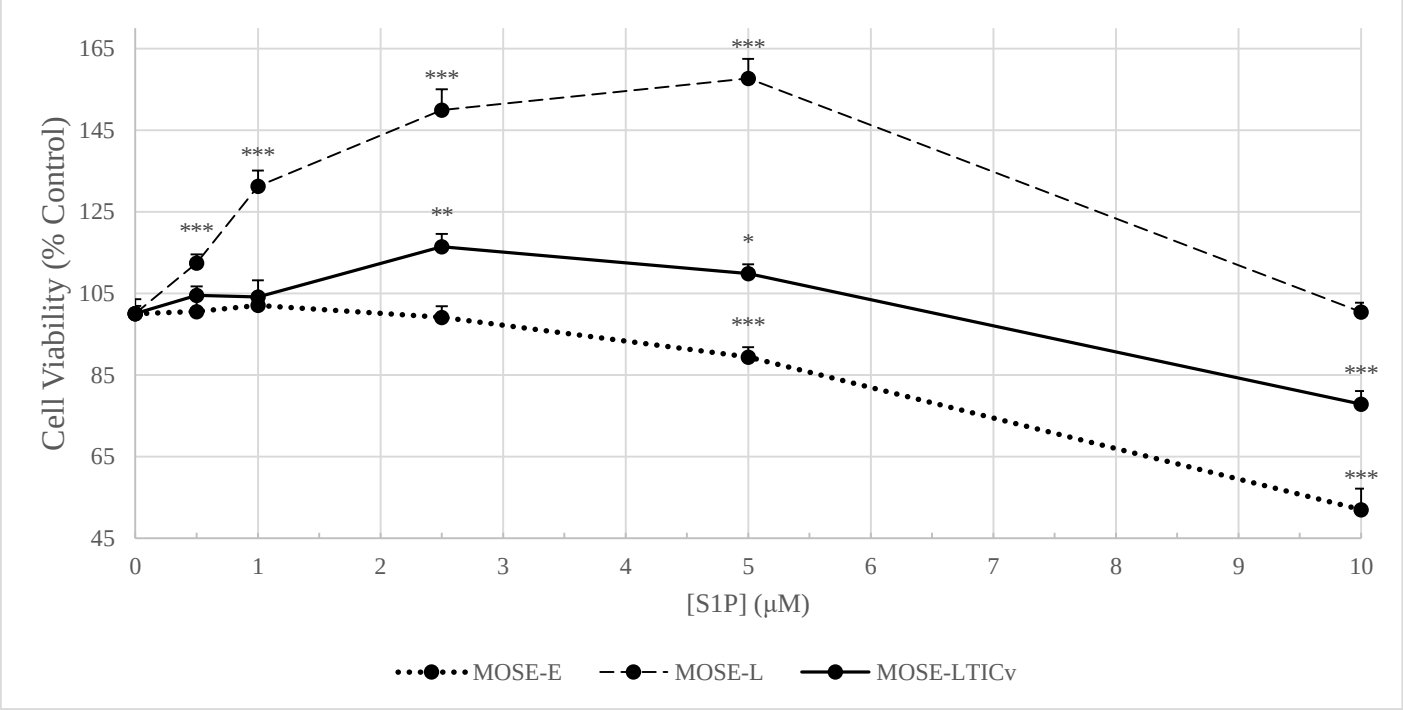

Figure 10. MTT Assay of adherent MOSE-E, MOSE-L, and MOSE-LTIC$_V$ cells after 72 hours of varying concentrations of S1P under hypoxic conditions. Viability was standardized as the percentage of the respective cell type control with BSA vehicle treatment. Significance was assessed using one-way ANOVA analysis (* indicates $p \leq 0.05$, ** indicates $p \leq 0.01$, *** indicates $p \leq 0.001$).

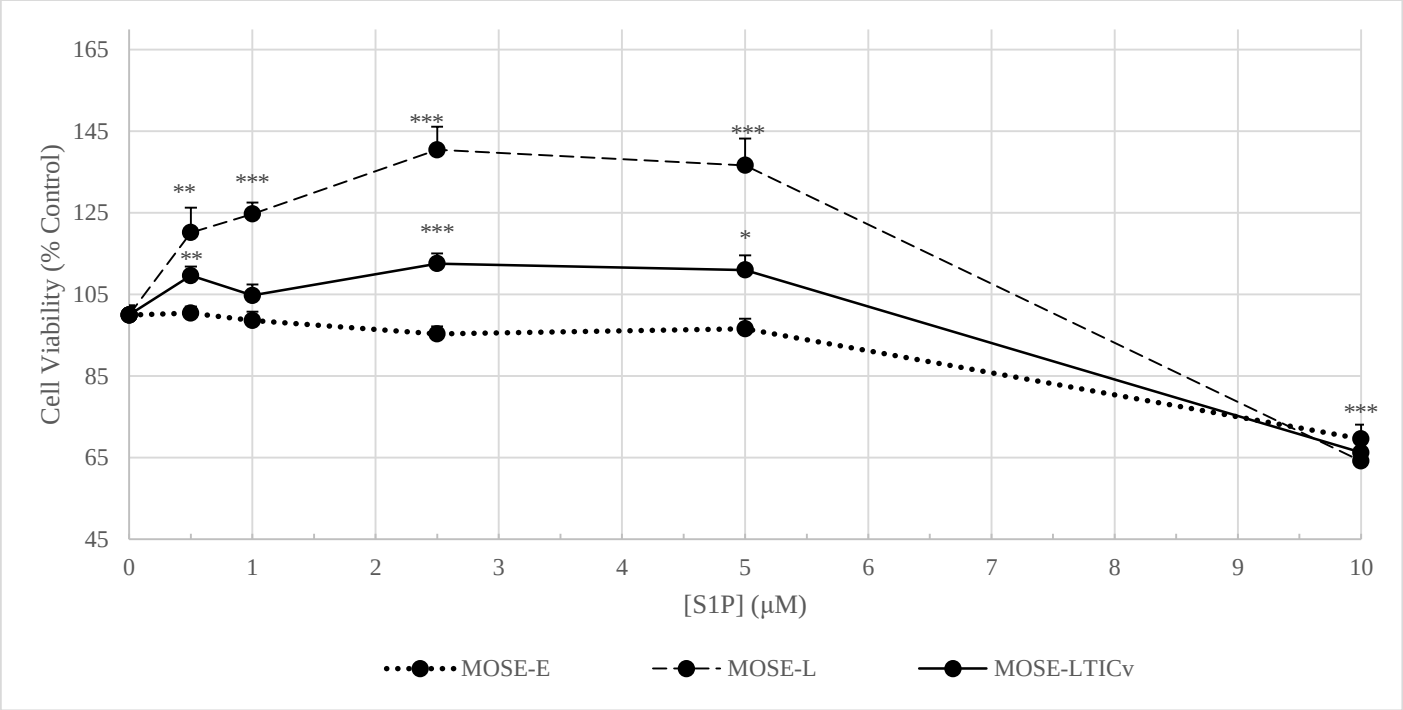

Figure 11. MTT Assay of adherent MOSE-E, MOSE-L, and MOSE-LTIC$_V$ cells after 72 hours of varying concentrations of S1P under normoxic conditions. Viability was standardized as the percentage of the respective cell type control with BSA vehicle treatment. Significance was assessed using one-way ANOVA analysis (* indicates $p \leq 0.05$, ** indicates $p \leq 0.01$, *** indicates $p \leq 0.001$).

In addition to the concentration dependency of the cellular response, we also performed a two-way ANOVA analysis to calculate the cell-type dependency of the response. We see a significant cell-type dependency compared to MOSE-E at specific concentrations in MOSE-L (normoxia: 0.5 μM [$p < 0.01$], 1.0, 2.5, 5.0 μM [$p < 0.0001$], 10 μM [ns]; hypoxia: 0.5 μM [$p < 0.01$], 1.0, 2.5, 5.0, 10 μM [$p < 0.0001$]) and MOSE-$_{LTICv}$ (normoxia: 0.5 μM [$p < 0.05$], 1.0 μM [ns], 2.5 μM [$p < 0.001$], 5.0 μM [$p < 0.01$], 10 μM [ns]; hypoxia: 0.5 μM [ns], 1.0 μM [ns], 2.5 μM [$p < 0.01$], 5.0 and 10 μM [$p < 0.001$]). This shows that the malignant MOSE cells respond both in a concentration and cell-type dependent manner to S1P, and this varies somewhat between hypoxia and normoxia.

S1P Increases the Size of MOSE-L Spheroids in Control Medium

Cancer spheroids are complex, compact structures that are inherently difficult in assessing viability. Several issues exist with using popular viability assays in spheroids,[46] and this issue may be exacerbated by spheroid size. Due to the longevity of these experiments resulting in very large spheroids that cannot be accurately assessed using these assays, spheroid size was selected as a marker of cell proliferation; however, the validity of this measure remains to be established as a reflection of spheroid viability. These experiments were done with control medium (DMEM-HG with 5% FBS).

Spheroid size measurements were taken of MOSE-L and MOSE-L^{TICv} spheroids at selected days after seeding: day 1, 5, 8, and 10. Under normoxia, MOSE-L cells exhibited a small—but significant—increase in spheroid size with 1 μM S1P treatment at days 5, 8, and 10 (Fig. 12). MOSE-L^{TICv} spheroids exhibited no significant change in spheroid size with S1P treatment. Both vehicle and treatment MOSE-L^{TICv} spheroids grew approximately 3 times larger than MOSE-L spheroid counterparts by Day 10 in normoxic conditions. However, under hypoxic conditions, MOSE-L spheroids retained a larger spheroid size than the respective MOSE-L^{TICv} spheroid groups (Fig. 13). Both cell lines experienced a decreased spheroid size under hypoxia compared to normoxia; however, this difference was dramatically different for the MOSE-L^{TICv} spheroids. Despite this decrease in spheroid size under hypoxia, MOSE-L spheroids retained the slight but significant increase in spheroid area after S1P treatment for 5, 8, and 10 days (Fig. 13). These results demonstrate that MOSE-L cells respond to S1P with an increase in spheroid size, suggesting that S1P may be implicated in the promotion of spheroid proliferation in the peritoneal cavity. MOSE-L^{TICv} spheroids did not respond to S1P supplementation, which was not surprising

due to their already incredibly metastatic and proliferative profile; similarly, they did not respond as strongly to S1P in an adherent monolayer as the MOSE-L cells (Figs. 10 and 11).

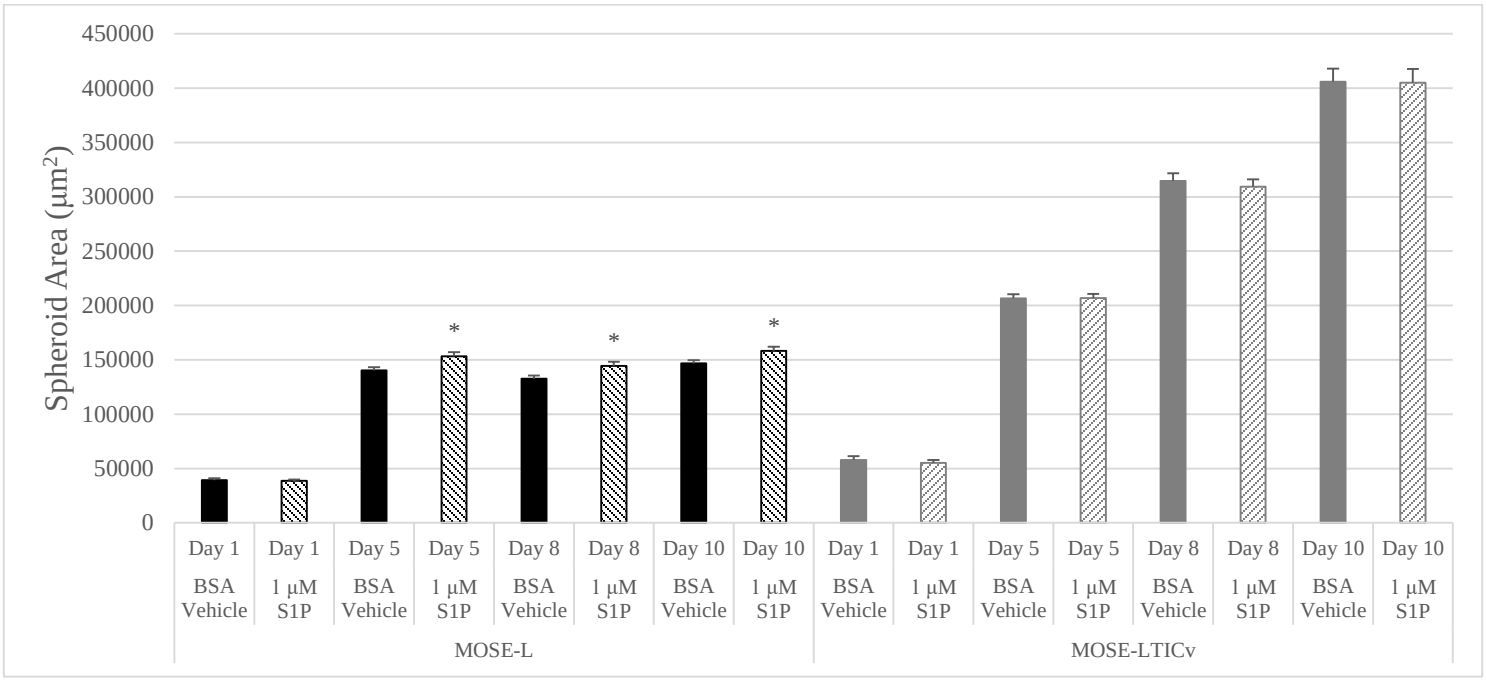

Figure 12. Impact of S1P on spheroid size of MOSE-L and MOSE-L^{TICv} cells under normoxia. Significance was assessed using one-way ANOVA analysis (* indicates $p \leq 0.05$).

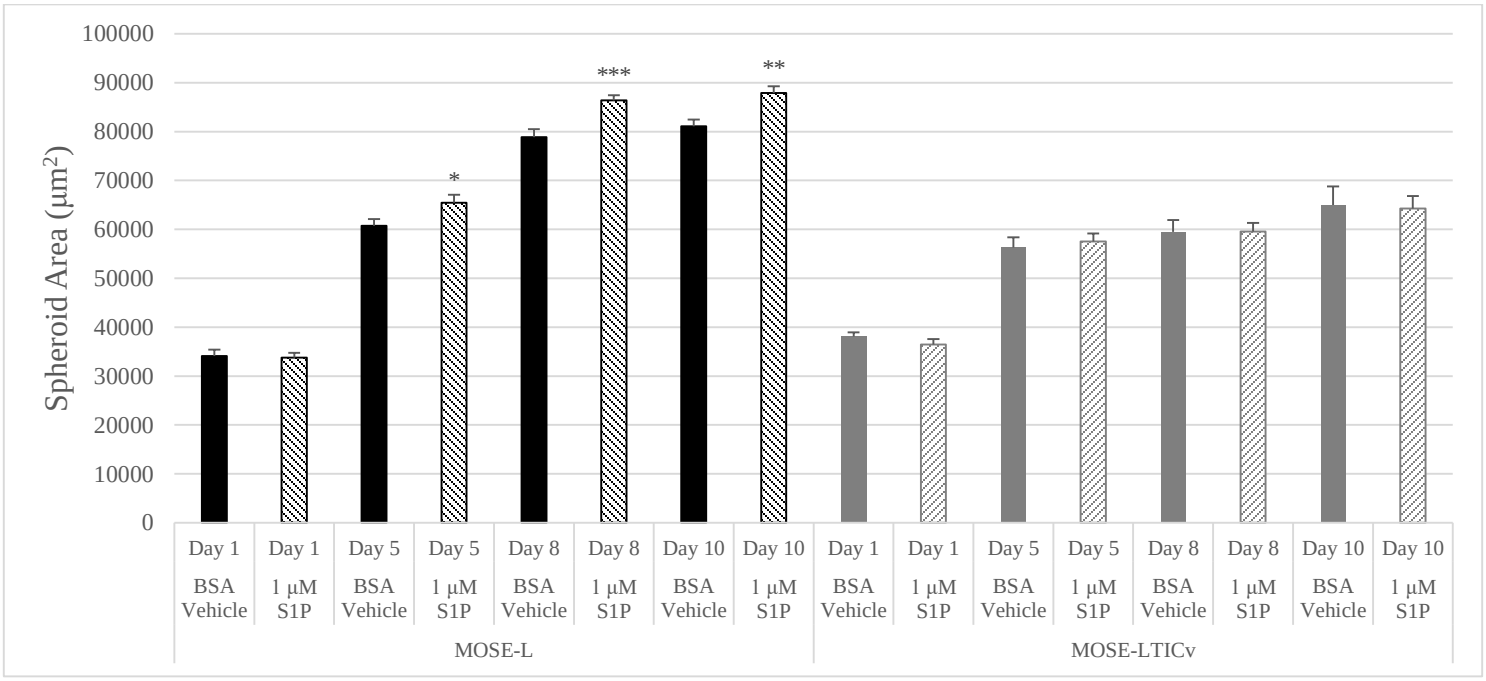

Figure 13. Impact of S1P on spheroid size of MOSE-L and MOSE-L^{TICv} cells under hypoxia. Significance was assessed using one-way ANOVA analysis (* indicates $p \leq 0.05$, ** indicates $p \leq 0.01$, *** indicates $p \leq 0.001$).

Impact of Stromal Cells on Cancer Cell Viability in Physiologically Relevant Conditions

Stromal cells isolated from HFD-fed, female C57BL/6 mice were investigated in heterogeneous MOSE-L and MOSE-L$_{TICv}$ spheroids under physiological conditions as rationalized in the introduction for their high SphK1 activity and tumor-promoting properties to potentially rescue the malignant cancer cells from a harsh environment similar to the peritoneal cavity. These nutrient-starved conditions are still relatively arbitrary, as a standard nutrient composition in the peritoneal cavity is not known and is variable. However, they may more accurately mimic physiological conditions compared to nutrient-rich medium. These cells were incorporated in a 2:1 MOSE:SVF cell ratio. Four conditions were assigned to both homogeneous cancer spheroids and heterogeneous cancer/stromal cell spheroids under both hypoxic and normoxic conditions: (1) control medium [5% FBS in DMEM-HG] (2) low-glucose (LG) medium [2 mM glucose in serum-free DMEM] (3) charcoal-stripped (CS) FBS medium [1% CS FBS in glucose-free DMEM] (4) serum-free, glucose-free DMEM. LG medium conditions are often not included in spheroid analyses in this paper to due to the strong proclivity of MOSE-L$_{TICv}$ spheroids to begin adhering to ultra-low adherence plates in this medium just one day after seeding. This behavior appears to be enhanced by the presence of stromal cells in the heterogeneous spheroids (Fig. 14). MOSE-L spheroids have less of an ability to adhere to these plates in the LG medium, although adherence of these cell spheroids has been documented in both homogeneous and heterogeneous spheroids, (Fig. 14) although it is not consistent. The mechanism and importance behind this adherence remains to be elucidated. Tables 1 and 2 summarize the conditions used throughout these experiments, and comparisons to established literature values.

	Control Medium	CS Medium	LG Medium	CS+LG Medium	-CS -LG Medium	Literature Values[29]
Type of Medium	DMEM-HG	DMEM	DMEM	DMEM	DMEM	-
% FBS	5%	-	-	-	-	-
% CS FBS	-	1%	-	1%	-	-
[Glucose]	25 mM	-	2 mM	2 mM	-	4.3 to 8.7 mM

Table 1. Medium formulations used in spheroid experiments.

	% O_2	**% CO_2**
Laboratory Normoxia	20%	5%
Laboratory Hypoxia	1%	5%
Range of Medians in Tumors[28]	0.3-4.2%	-
Range of Medians in Normal Tissue[28]	3.4-6.8%	-

Table 2. Percent oxygen and carbon dioxide values used in experiments and compared to literature values.

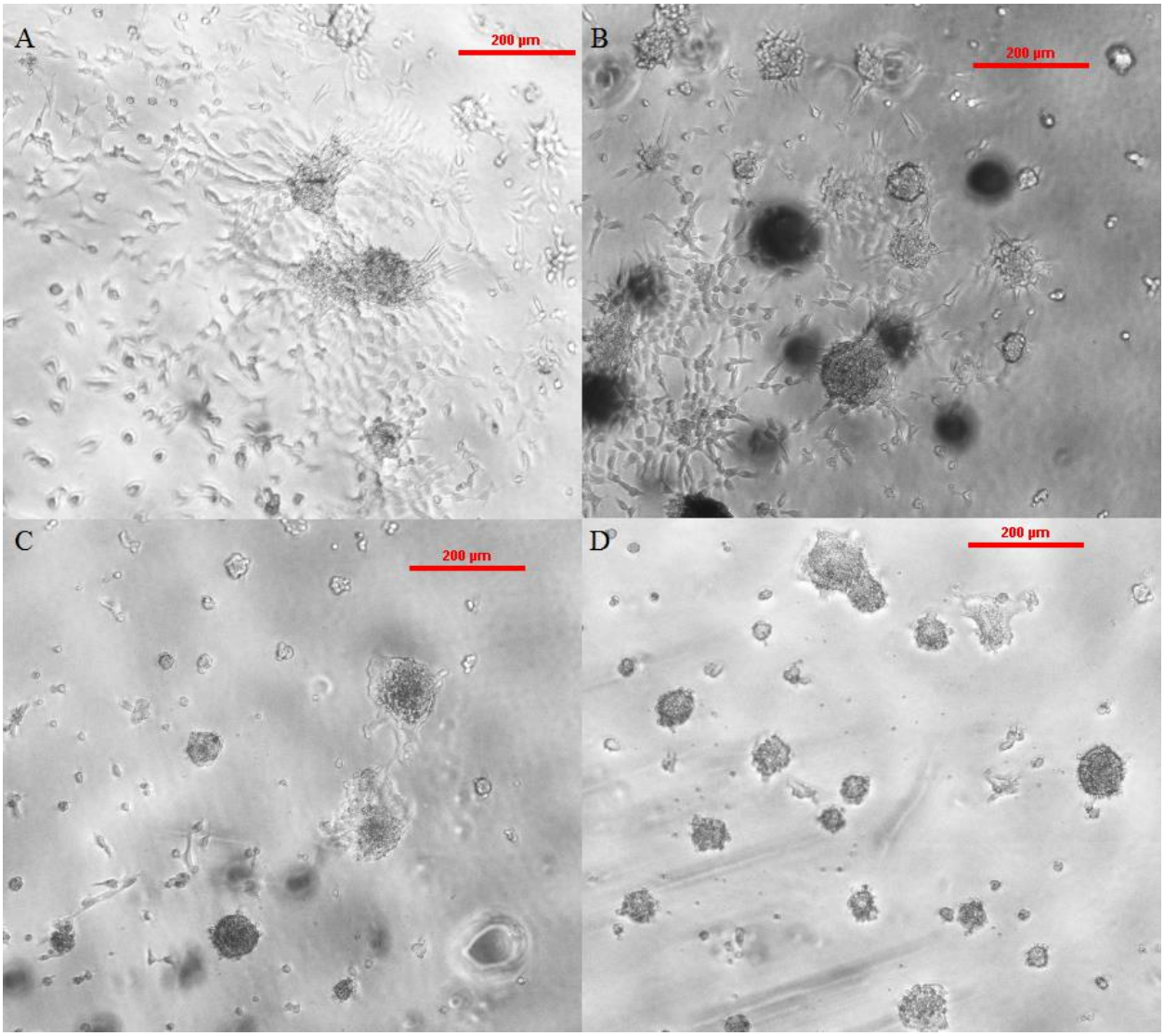

Figure 14. Images of spheroid adhesion to ultra-low adherence plates in 2 mM glucose serum-free medium with (A) heterogeneous MOSE-L$_{TICv}$ + SVF (B) homogeneous MOSE-L$_{TICv}$ (C) heterogeneous MOSE-L + SVF (D) homogeneous MOSE-L spheroids. Images from timepoint Day 1.

Heterogeneous MOSE-L spheroids exhibited a significantly increased spheroid size at days 5, 8, and 10 in normoxic conditions with the control medium compared to homogeneous spheroids (Fig. 15). This is consistent with our hypothesis that stromal cells contribute to enhanced spheroid proliferation when co-cultured. Unexpectedly, however, there was no change in any of the nutrient deprived conditions under normoxia with the incorporation of stromal cells into the cancer spheroids, except for a significant decrease in spheroid size of the heterogeneous spheroids in LG

medium glucose (Fig. 15). Under hypoxic conditions, MOSE-L spheroids showed a similar significant increased spheroid size at days 5, 8, and 10 in the control medium compared to homogeneous counterparts (Fig. 16). Interestingly, at day 1, the heterogeneous spheroids are significantly smaller than the homogeneous spheroids in hypoxia, despite a rapid growth that outpaces the homogeneous spheroids through the course of the experiment, suggesting a role of these cells in spheroid proliferation under nutrient-rich conditions. In hypoxia—similar to normoxia—the heterogeneous composition has no impact on spheroid size in any of the nutrient-deprived groups. Heterogeneous spheroids in CS medium exhibited a smaller initial size at day 1, which grew to levels comparable to homogeneous controls at days 5, 8, and 10. Furthermore, heterogeneous no-glucose no-serum spheroids were significantly smaller at all points of the experiment. Spheroids in LG medium were excluded from size analyses due to some adherence, particularly later in the experiment (day 5 onward). While MOSE+SVF co-culturing increased spheroid size in control medium as we hypothesized, the results from the nutrient-deprived medium conditions demonstrate that stromal cells cannot rescue spheroid growth in these more physiologically relevant environments, whether under hypoxia or normoxia. This indicates that stromal cells may be implicated in another function in ovarian cancer progression and metastasis rather than spheroid proliferation.

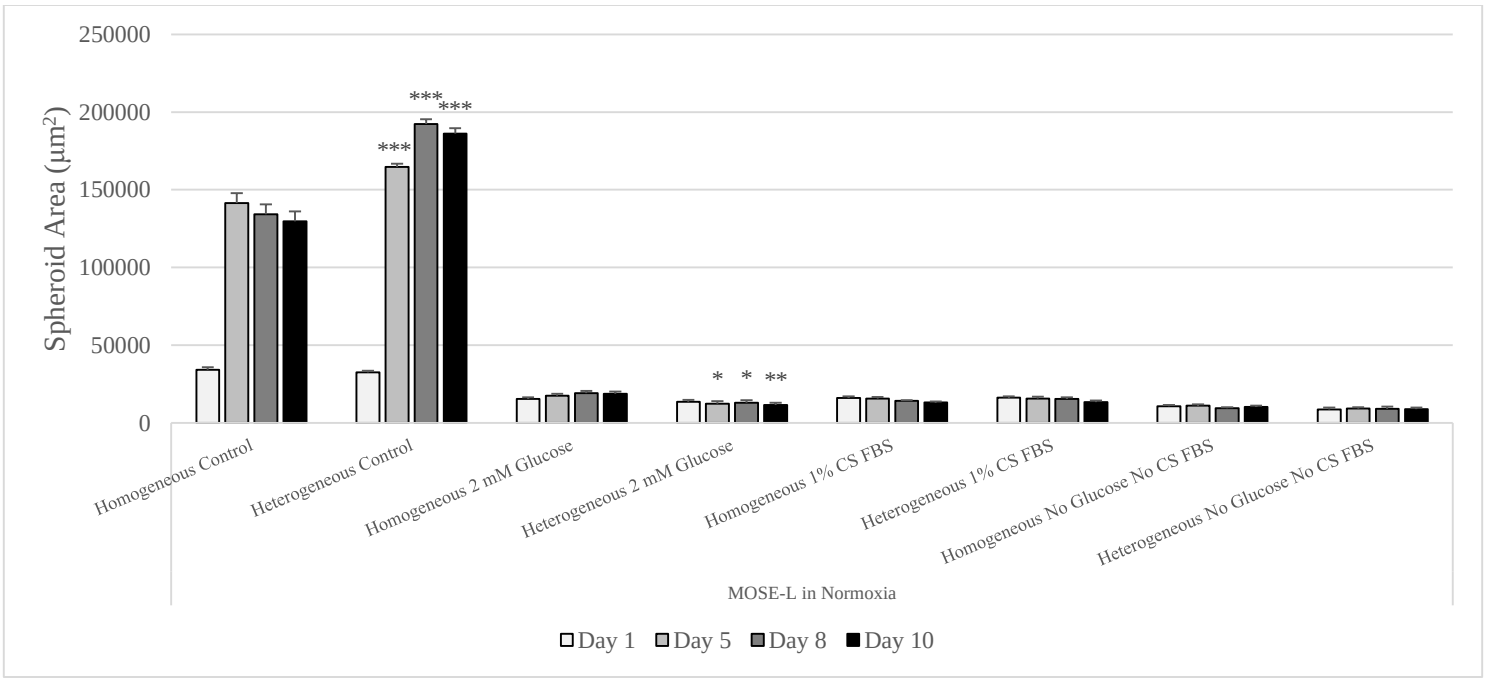

Figure 15. Spheroid size analysis of several different treatment groups with homogeneous MOSE-L spheroids compared to heterogeneous MOSE-L + SVF spheroids under normoxic conditions. Significance was assessed using one-way ANOVA analysis (* indicates $p \leq 0.05$, ** indicates $p \leq 0.01$, *** indicates $p \leq 0.001$).

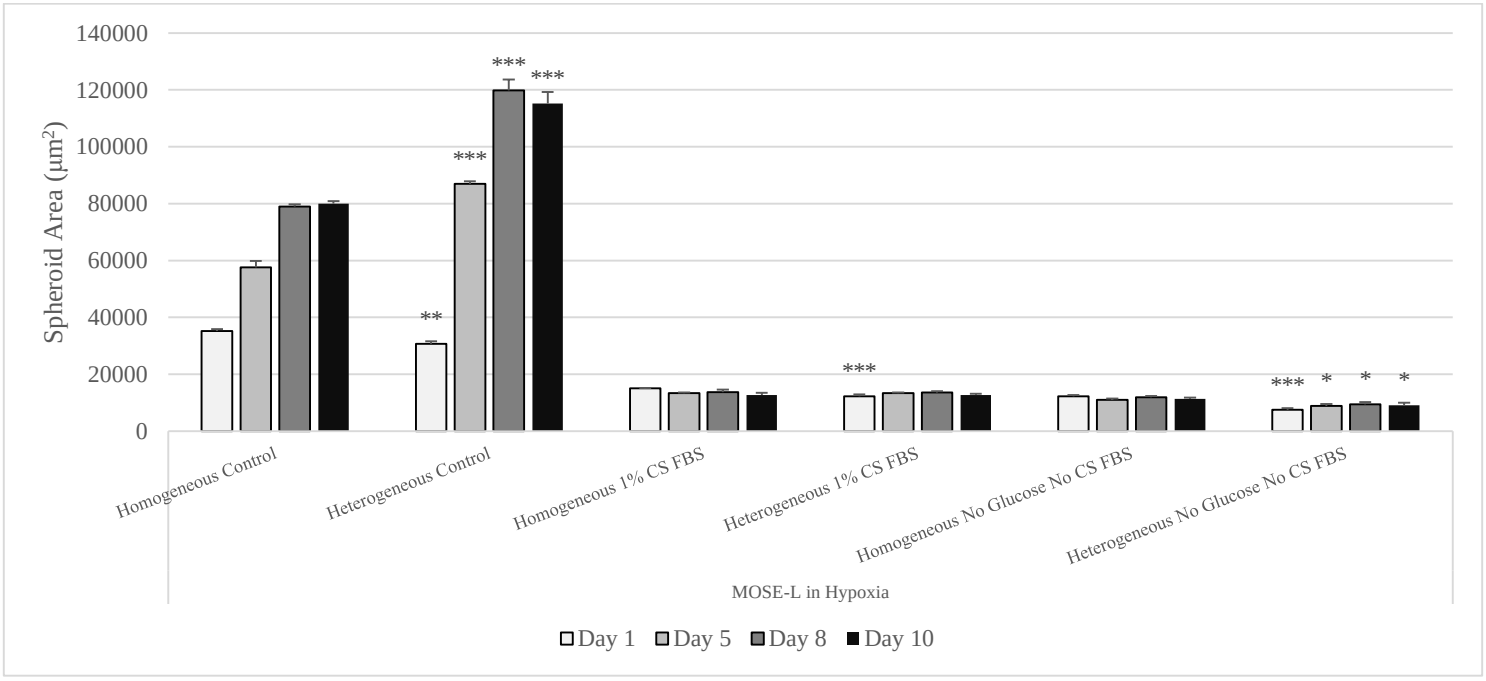

Figure 16. Spheroid size analysis of several different treatment groups with homogeneous MOSE-L spheroids compared to heterogeneous MOSE-L + SVF spheroids under hypoxic conditions. Significance was assessed using one-way ANOVA analysis (* indicates $p \leq 0.05$, ** indicates $p \leq 0.01$, *** indicates $p \leq 0.001$).

MOSE-L$_{TICv}$ spheroid size responded minimally to the incorporation of stromal cells. In normoxia, there was no change in spheroid size at any time point beyond day 1 (Fig. 17). At day 1, the heterogeneous spheroids in control medium and spheroids in LG medium were significantly smaller than the homogeneous spheroids; however, these spheroids normalized over time to their homogeneous counterparts. In hypoxic conditions, there was a significant increase in spheroid size at day 5 in the heterogeneous spheroids with control medium after a significantly decreased spheroid size at day 1 (Fig. 18). However, at days 8 and 10, there was no observable difference in heterogeneous spheroid size in control medium. Heterogeneous spheroids in CS medium were significantly smaller than homogeneous spheroids at day 10. Spheroids in LG medium were excluded from size analyses due to extensive adherence in hypoxic conditions. These results were inconsistent with our original hypothesis as also described in the MOSE-L spheroid analysis. Stromal cells do not rescue the MOSE-L$_{TICv}$ spheroids in any of the starved conditions (or nutrient-rich condition representing physiologically relevant conditions. However, stromal cells may be implicated in other facets of ovarian cancer progression. The summary of the effects of SVF co-culturing on MOSE-L and MOSE-L$_{TICv}$ spheroid size are shown in Table 3.

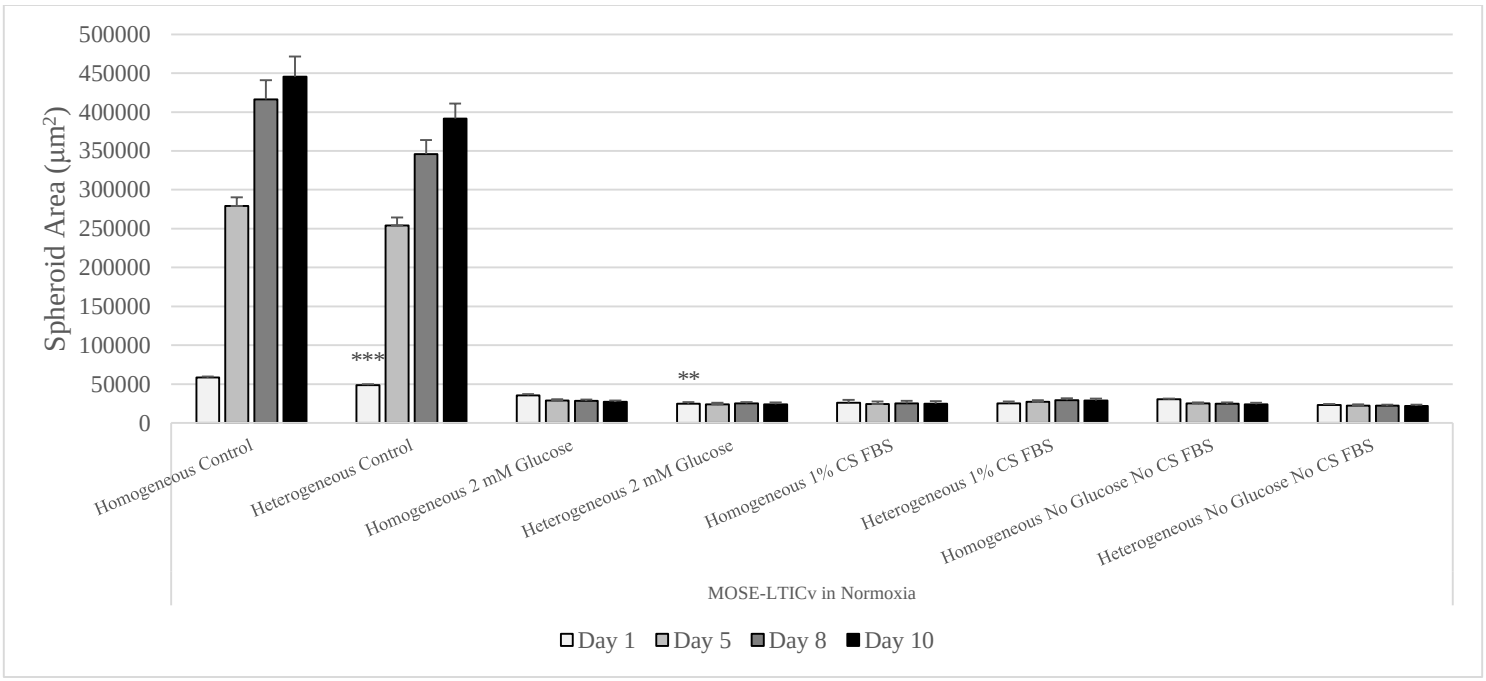

Figure 17. Spheroid size analysis of several different treatment groups with homogeneous MOSE-L spheroids compared to heterogeneous MOSE-LTICv + SVF spheroids under normoxic conditions. Significance was assessed using one-way ANOVA analysis (** indicates $p \leq 0.01$, *** indicates $p \leq 0.001$).

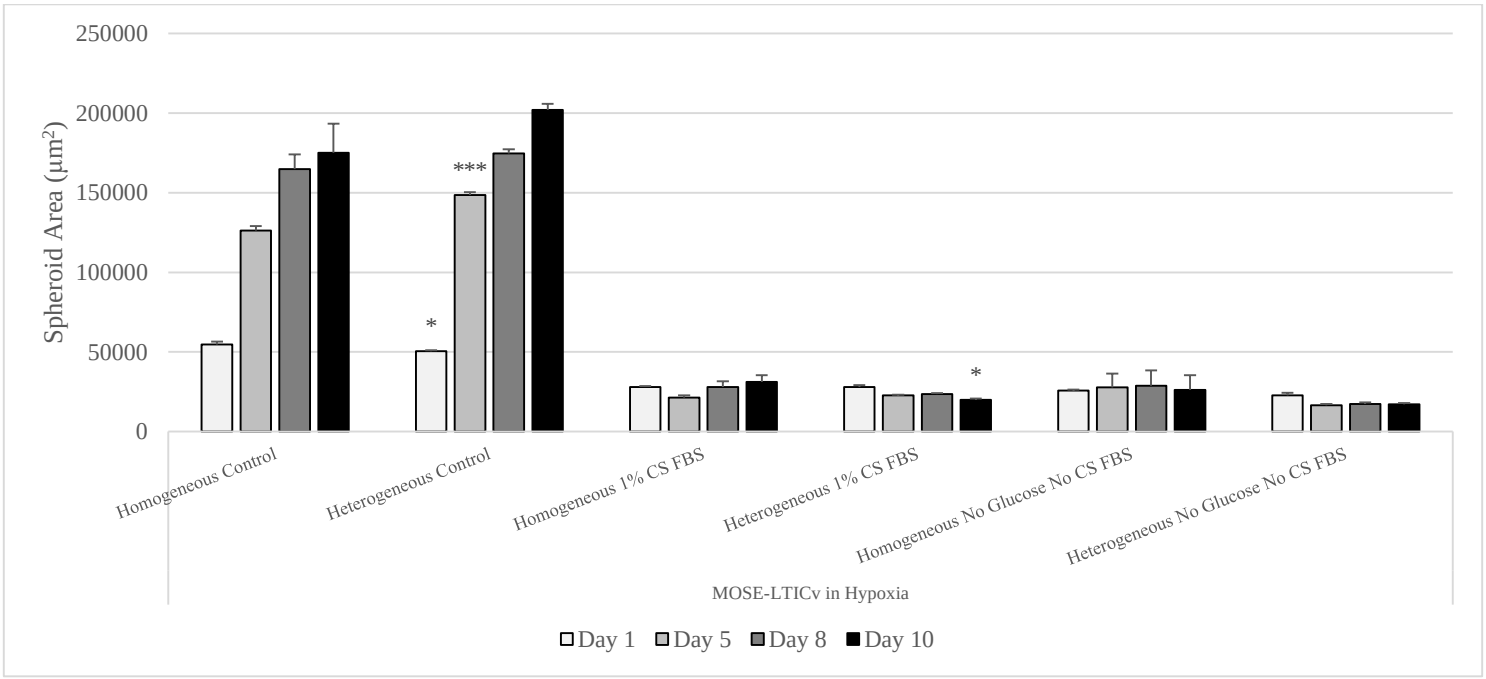

Figure 18. Spheroid size analysis of several different treatment groups with homogeneous MOSE-L spheroids compared to heterogeneous MOSE-LTICv + SVF spheroids under hypoxic conditions. Significance was assessed using one-way ANOVA analysis (* indicates $p \leq 0.05$, *** indicates $p \leq 0.001$).

Co-Culture	Normoxia		Hypoxia	
	MOSE-L	MOSE-L_{TICv}	MOSE-L	MOSE-L_{TICv}
Control Medium	⇧	▭	⇧	▭
LG Medium	⇩	▭	▭	▭
CS Medium	▭	▭	▭	⇩
-CS -LG Medium	▭	▭	⇩	▭

Table 3. Summary of the impact of SVF cells on MOSE spheroid growth when co-cultured under varying conditions using day 10 measurements compared to controls. ⇧ = Increase in size, ⇩ = decrease, ▭ = no change.

S1P Does Not Rescue Cancer Cell Viability in Nutrient-Starved Conditions

Since the stromal cells did not elicit a protective or proliferative function in heterogeneous spheroids in starved conditions, 1 μM S1P was re-introduced to potentially stimulate a more potent proliferative response, as shown in the MOSE-L cells under control medium previously. Furthermore, completely starved medium (no glucose, no charcoal-stripped FBS) was decided to be too unphysiological of an environment for subsequent analysis and was replaced with DMEM that contained both 2 mM glucose and 1% charcoal-stripped FBS (LG+CS medium). However, in both hypoxia and normoxia for MOSE-L and MOSE-L_{TICv} spheroids, there was no change in any spheroid size in any of the starved conditions (Figs. 19-22). The MOSE-L spheroids show a similar trend for an increased spheroid size in MOSE-L under both hypoxia and normoxia with S1P treatment. Unexpectedly, S1P does not rescue MOSE spheroid growth in starved conditions, as seen with the SVF cell co-culturing. These results indicate that S1P is not implicated in spheroid proliferation in physiologically relevant conditions for MOSE-L and MOSE-L_{TICv} spheroids. Thus, if S1P is supporting MOSE spheroid metastatic potential, it is not via increased proliferation. Neither S1P nor SVF cells rescue malignant spheroids in either hypoxia or normoxia in any of the

nutrient-starved conditions. The summary of the effects of S1P supplementation on MOSE-L and MOSE-L$_{TICv}$ spheroid size are shown in Table 4.

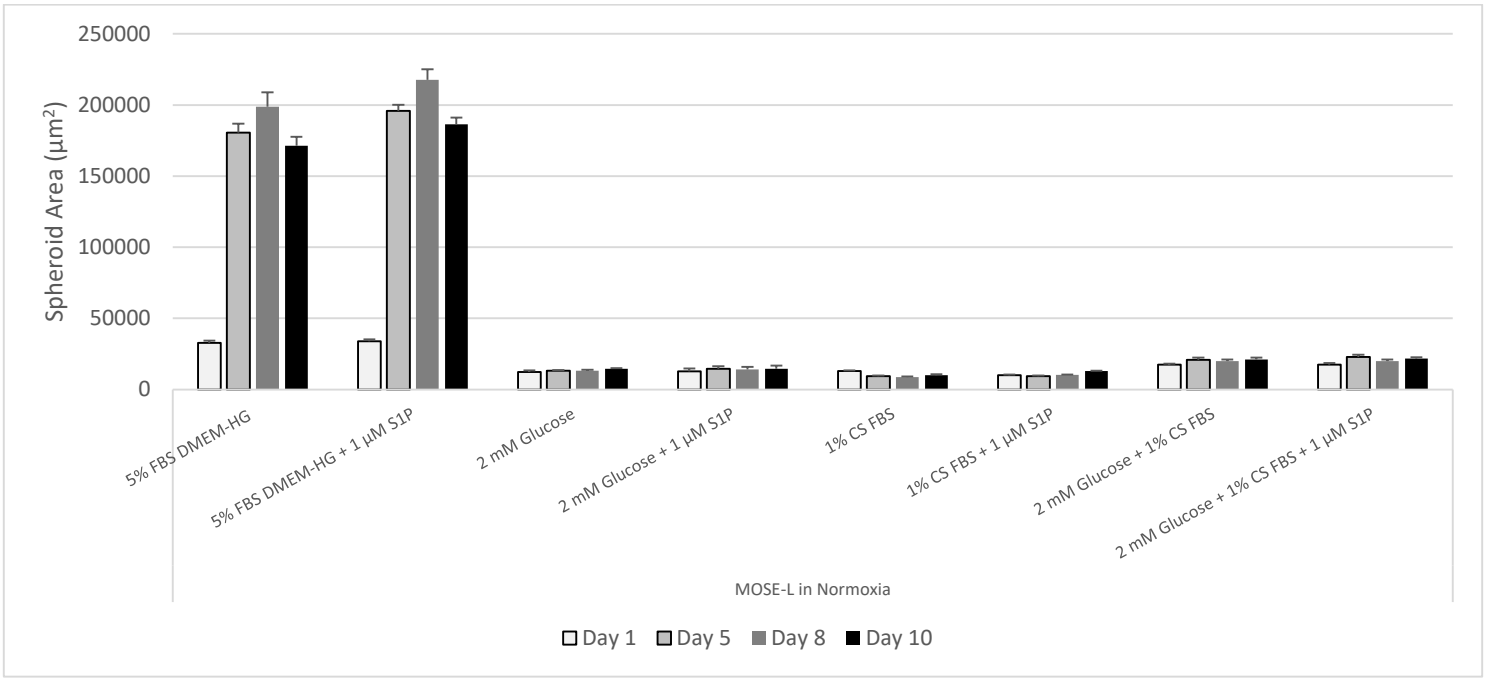

Figure 19. Spheroid size analysis of several different treatment groups of MOSE-L cells with BSA vehicle or 1 µM S1P under normoxia. Significance was assessed using one-way ANOVA analysis.

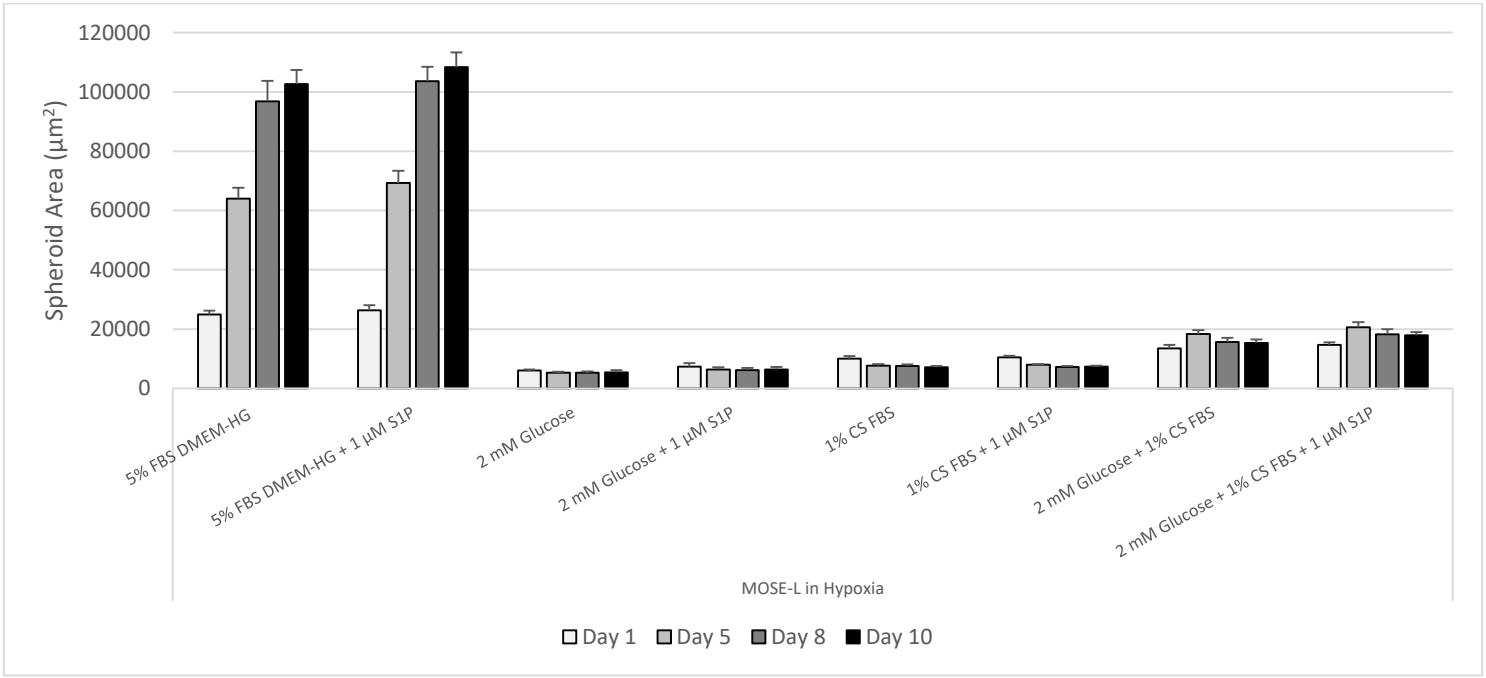

Figure 20. Spheroid size analysis of several different treatment groups of MOSE-L cells with BSA vehicle or 1 µM S1P under hypoxia. Significance was assessed using one-way ANOVA analysis.

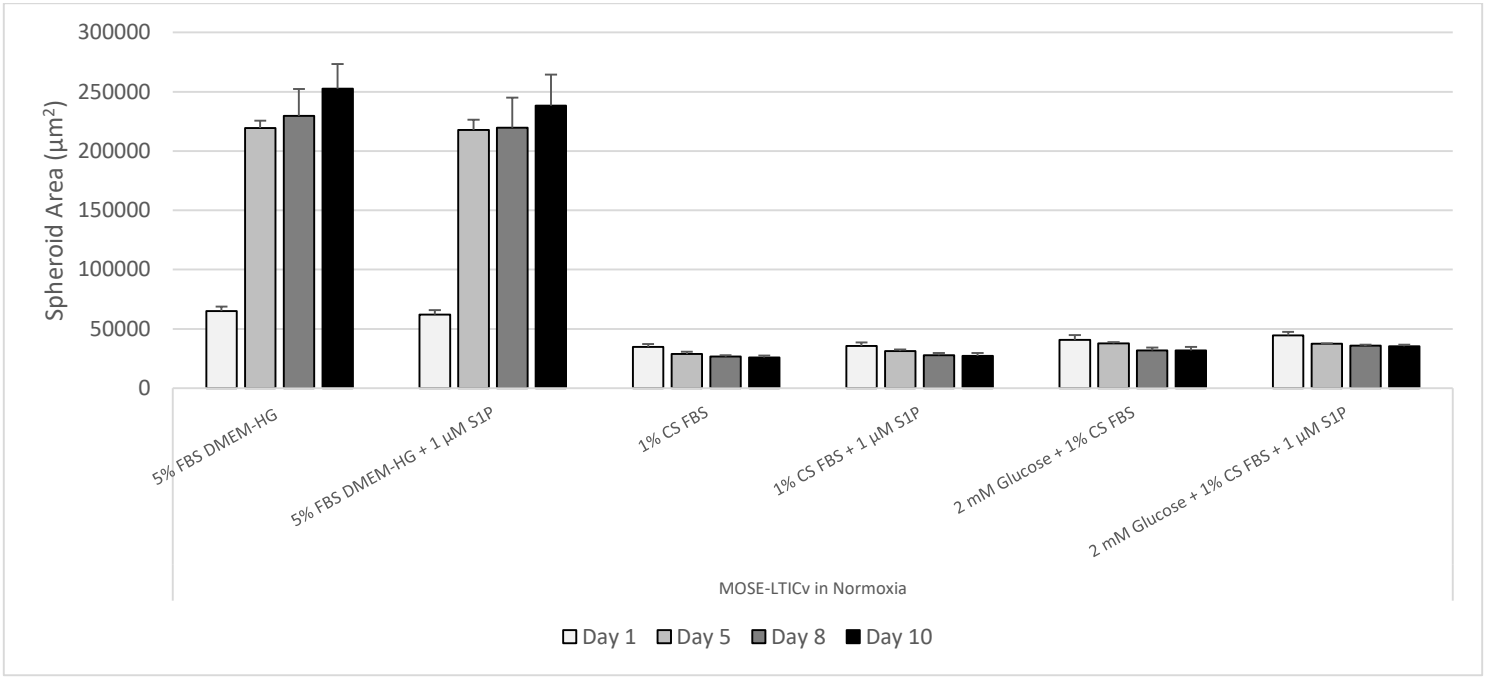

Figure 21. Spheroid size analysis of several different treatment groups of MOSE-LTICv cells with BSA vehicle or 1 µM S1P under normoxia. Significance was assessed using one-way ANOVA analysis.

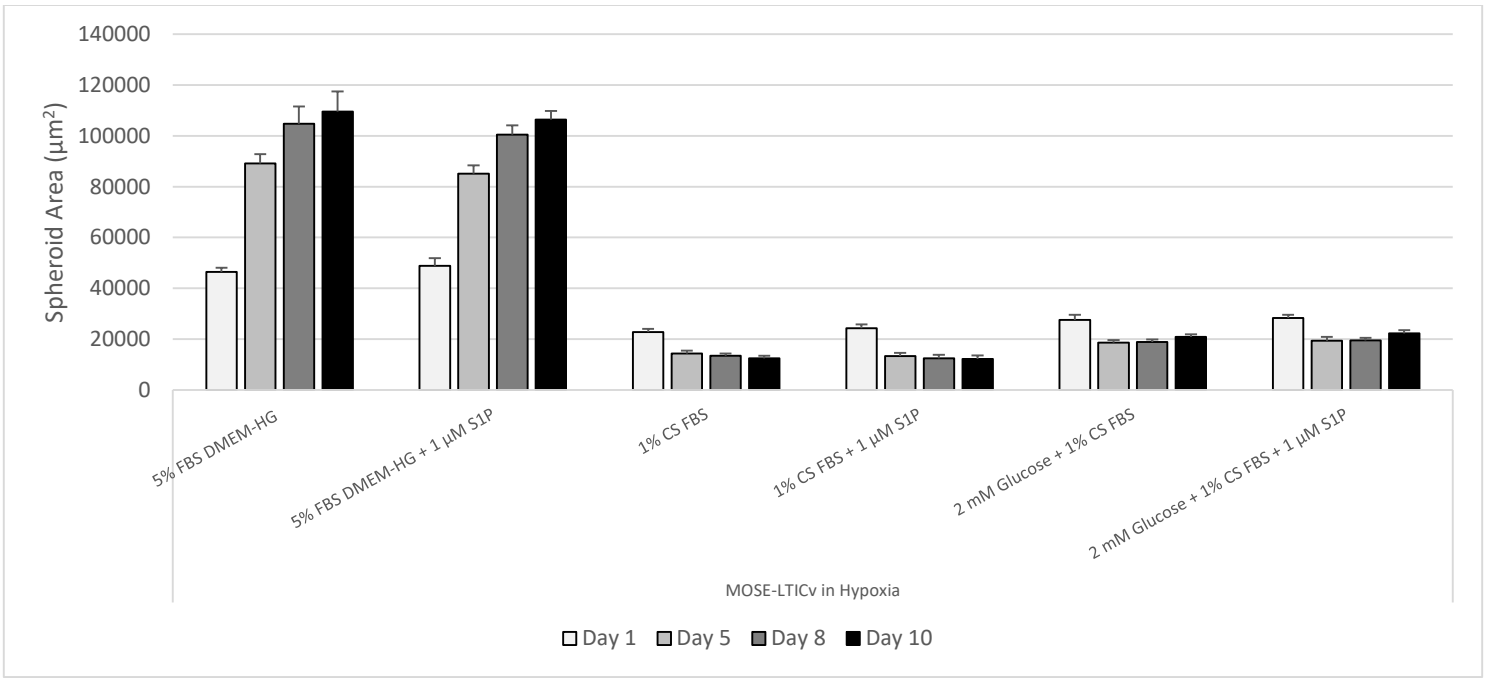

Figure 22. Spheroid size analysis of several different treatment groups of MOSE-LTICv cells with BSA vehicle or 1 µM S1P under hypoxia. Significance was assessed using one-way ANOVA analysis.

S1P	Normoxia		Hypoxia	
	MOSE-L	MOSE-L_{TICv}	MOSE-L	MOSE-L_{TICv}
Control Medium	⇧	▭	⇧	▭
LG Medium	▭	▭	▭	▭
CS Medium	▭	▭	▭	▭
+CS +LG Medium	▭	▭	▭	▭

Table 4. Summary of the impact of S1P on MOSE spheroid growth when co-cultured under varying conditions using day 10 measurements compared to controls. ⇧ = Increase in size, ⇩ = decrease, ▭ = no change.

Effect of Hypoxic Environments and Stromal Cell Incorporation on MOSE Outgrowth

After MOSE-L and MOSE-L_{TICv} spheroids were treated with S1P or co-cultured with stromal cells in heterogeneous spheroids for 5 days, they were transferred to 48-well tissue-culture treated plates and analyzed for adhesion/outgrowth after 24 hours since spheroid size might not be the best biological read-out for physiological responses to treatment conditions. MOSE-L_{TICv} spheroids are the focal point of this section due to their adherence in each of the nutrient-deprived conditions—MOSE-L spheroids only consistently adhered and had considerable outgrowth in control medium and, therefore, did not result in a robust outgrowth in any of the nutrient-starved conditions.

The impact of oxygen level on outgrowth area for heterogeneous and homogeneous MOSE-L_{TICv} spheroids is dependent on the various medium conditions. In both spheroid types, there is a decrease in total outgrowth area in control medium (Figs. 23 and 24) in hypoxic conditions; however, in homogeneous spheroids, there is an increased outgrowth area in hypoxia with LG+CS medium (Fig. 20) and in heterogeneous spheroids, there is an increased outgrowth in LG medium in addition to CS medium (Fig. 21). These differences highlight the importance of

using physiologically relevant conditions, as analyses in nutrient-rich, normoxic conditions show entirely different responses than in nutrient-starved, hypoxic conditions.

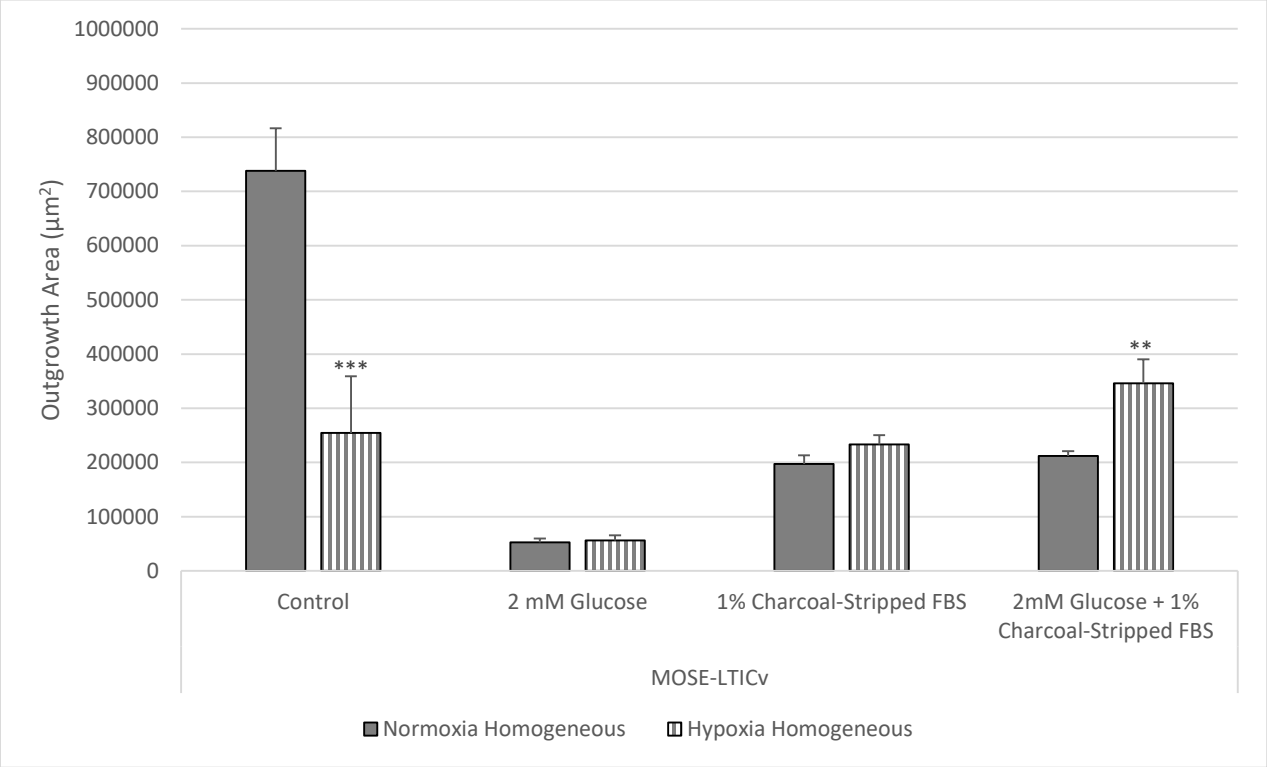

Figure 23. Comparison of spheroid outgrowth of homogeneous MOSE-LTICv spheroid outgrowth in normoxia and hypoxia. Significance was assessed using one-way ANOVA analysis (** indicates $p \leq 0.01$, *** indicates $p \leq 0.001$).

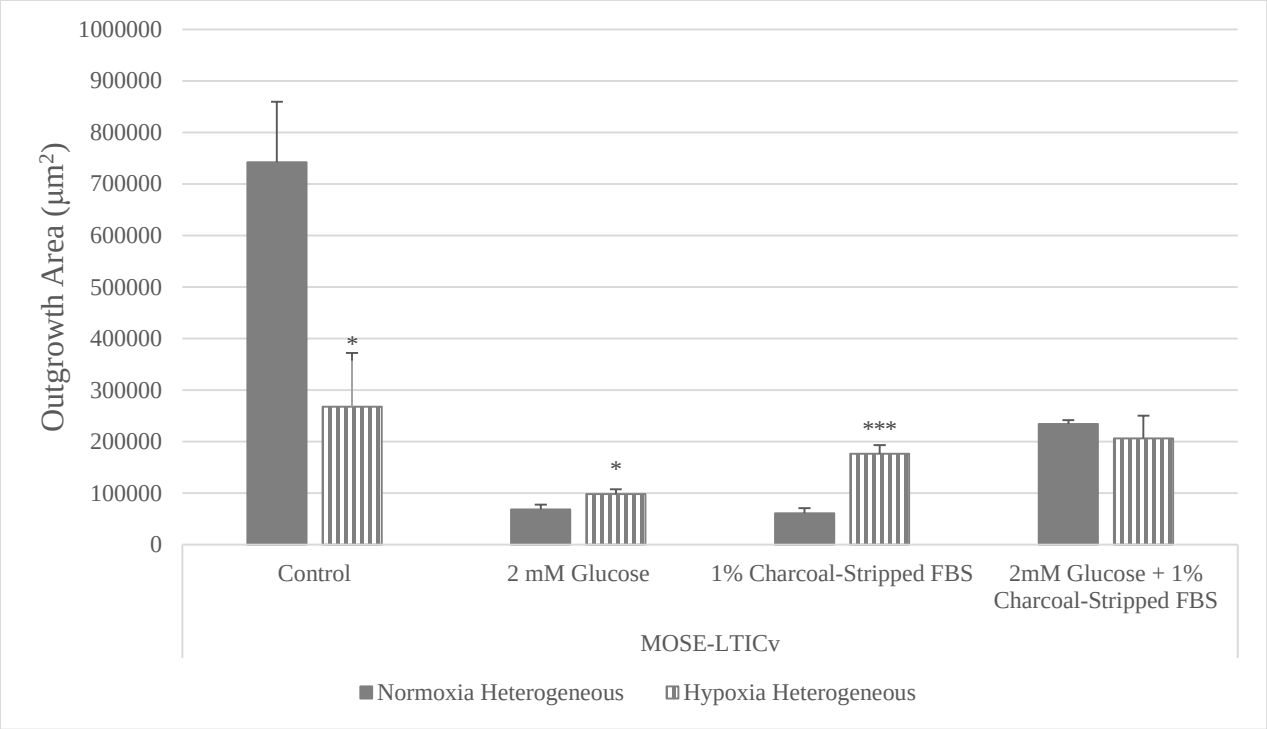

Figure 24. Comparison of spheroid outgrowth of heterogeneous MOSE-LTICv spheroid outgrowth in normoxia and hypoxia. Significance was assessed using one-way ANOVA analysis (* indicates $p \leq 0.05$, *** indicates $p \leq 0.001$).

Heterogeneity of the spheroids appears to have little effect on the outgrowth area of MOSE-LTICv spheroids. Under normoxia, the outgrowth is not different between groups, except for a significant decrease in outgrowth area in the CS medium (Fig. 25) which suggests a reliance on glucose in the medium for heterogeneous spheroids. In hypoxia, however, the outgrowth area is significantly increased with heterogeneous spheroids compared to homogeneous spheroids in LG medium; moreover, there is a significant decrease in outgrowth in the CS medium and LG+CS medium (Fig. 26). These results indicate that, except for LG, hypoxic conditions, SVF co-culturing had no effect on MOSE-LTICv outgrowth area. This was not consistent with our hypothesis that stromal cells are implicated in ovarian cancer adhesion and progression of these highly malignant cells, although the LG hypoxia condition did show a significant effect of stromal cells in increasing outgrowth compared to homogeneous

counterparts. The summary of the change in outgrowth area from co-culturing is shown in Table 5.

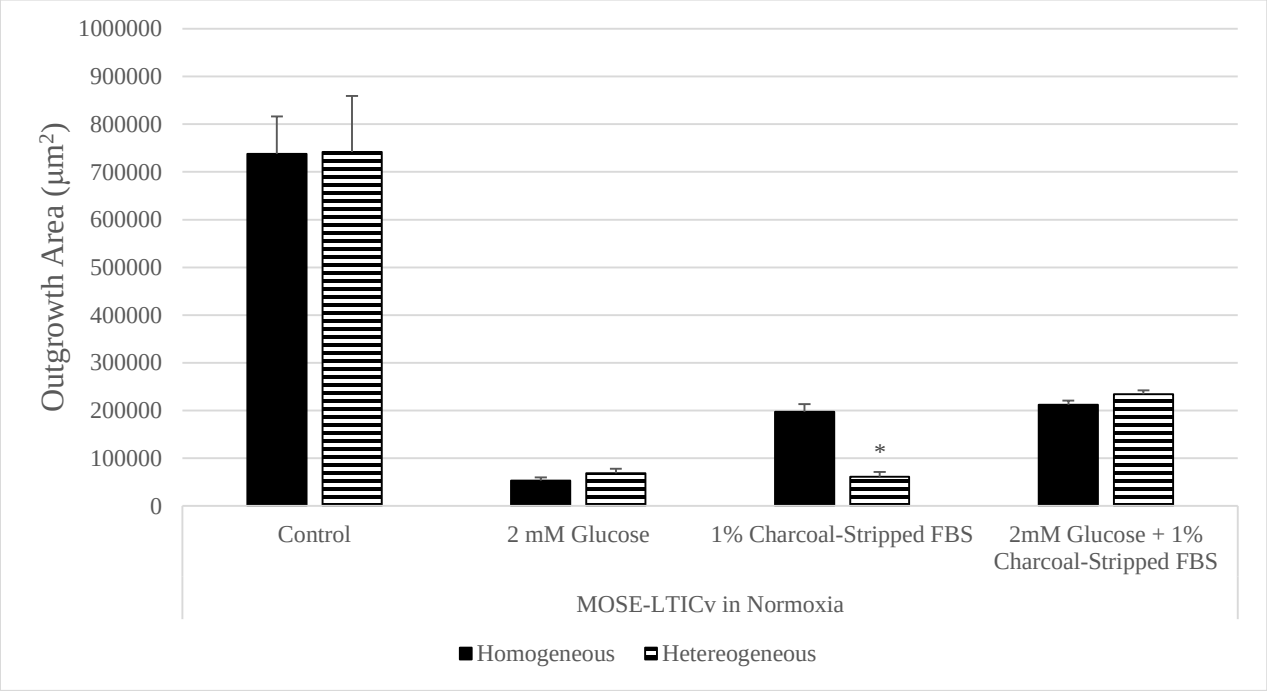

Figure 25. Comparison homogeneous and heterogeneous MOSE-L^{TICv} spheroid outgrowth in normoxia. Significance was assessed using one-way ANOVA analysis (* indicates $p \leq 0.05$).

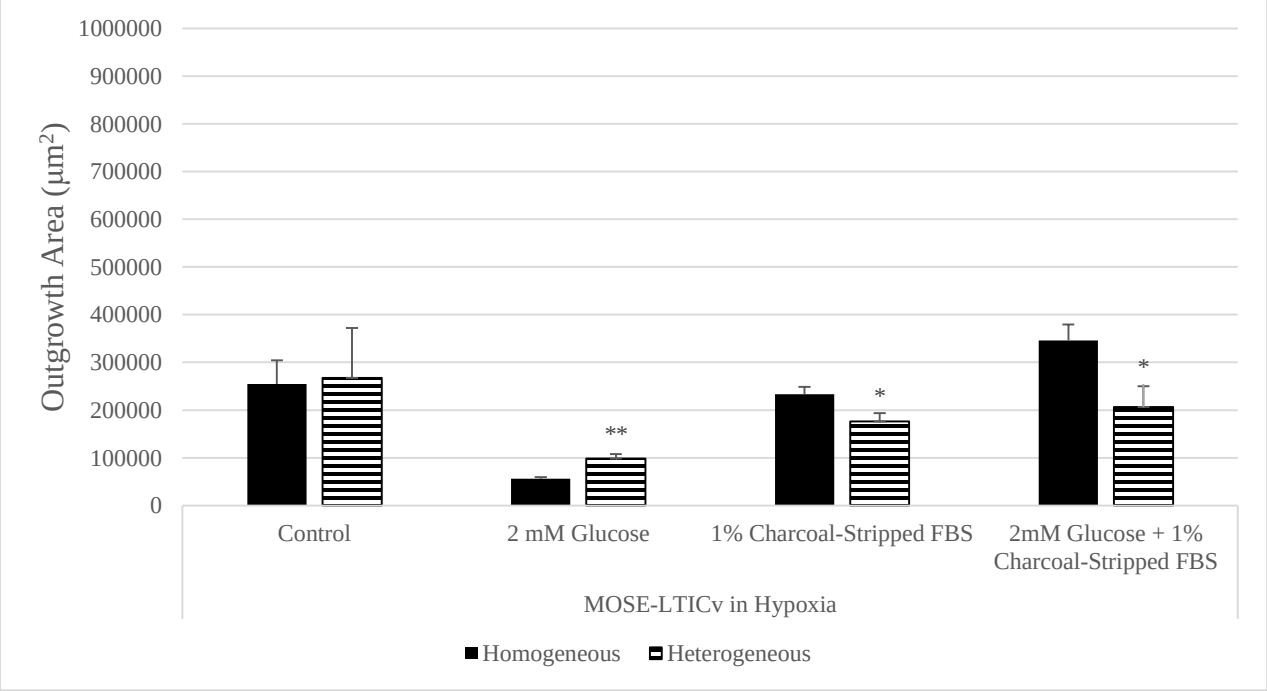

Figure 26. Comparison of homogeneous and heterogeneous MOSE-L^{TICv} spheroid outgrowth in hypoxia. Significance was assessed using one-way ANOVA analysis (* indicates $p \leq 0.05$, ** indicates $p \leq 0.01$).

Co-culture	Normoxia	Hypoxia
	MOSE-L_{TICv}	MOSE-L_{TICv}
Control Medium	▭	▭
LG Medium	▭	⇧
CS Medium	⇩	⇩
+CS +LG Medium	▭	⇩

Table 5. Summary of the impact of SVF cells on MOSE spheroid outgrowth when co-cultured under varying conditions using 24 hour measurements compared to controls. ⇧ = Increase in outgrowth, ⇩ = decrease, ▭ = no change.

Effect of Hypoxic Environments and S1P Supplementation on MOSE-L_{TICv} Outgrowth

Homogeneous BSA vehicle- or S1P-treated MOSE-L_{TICv} spheroids exhibited a lower outgrowth area under hypoxic conditions in control medium (Figs. 27 and 28) and—consistent with the previously discussed homogeneous spheroids—had an increased outgrowth in CS and LG+CS medium in hypoxia. This furthermore highlights the variability of results between hypoxic and normoxic conditions, as seen previously. Again, these results show the importance of using physiological culture conditions to produce relevant results.

S1P supplementation had no effect on outgrowth area under normoxia (Fig. 29). In hypoxia, however, S1P supplementation significantly increased the outgrowth of MOSE-L_{TICv} spheroids in LG medium—similar to what was seen with SVF co-culturing—and significantly decreased the outgrowth of spheroids in LG+CS medium (Fig. 30). These results are similar to the SVF co-culturing results in that S1P supplementation did not result in an increased outgrowth of MOSE-L_{TICv} spheroids—except in LG medium in hypoxia. Taken together, these results show

that neither stromal cells nor S1P had a significant impact on outgrowth of MOSE-LTICv spheroids, except in LG hypoxic conditions. While we did observe this significant increase in growth under LG hypoxic conditions, these responses were not as robust as we expected across the many conditions. The impact of S1P supplementation on spheroid growth of MOSE-LTICv spheroids is summarized in Table 6.

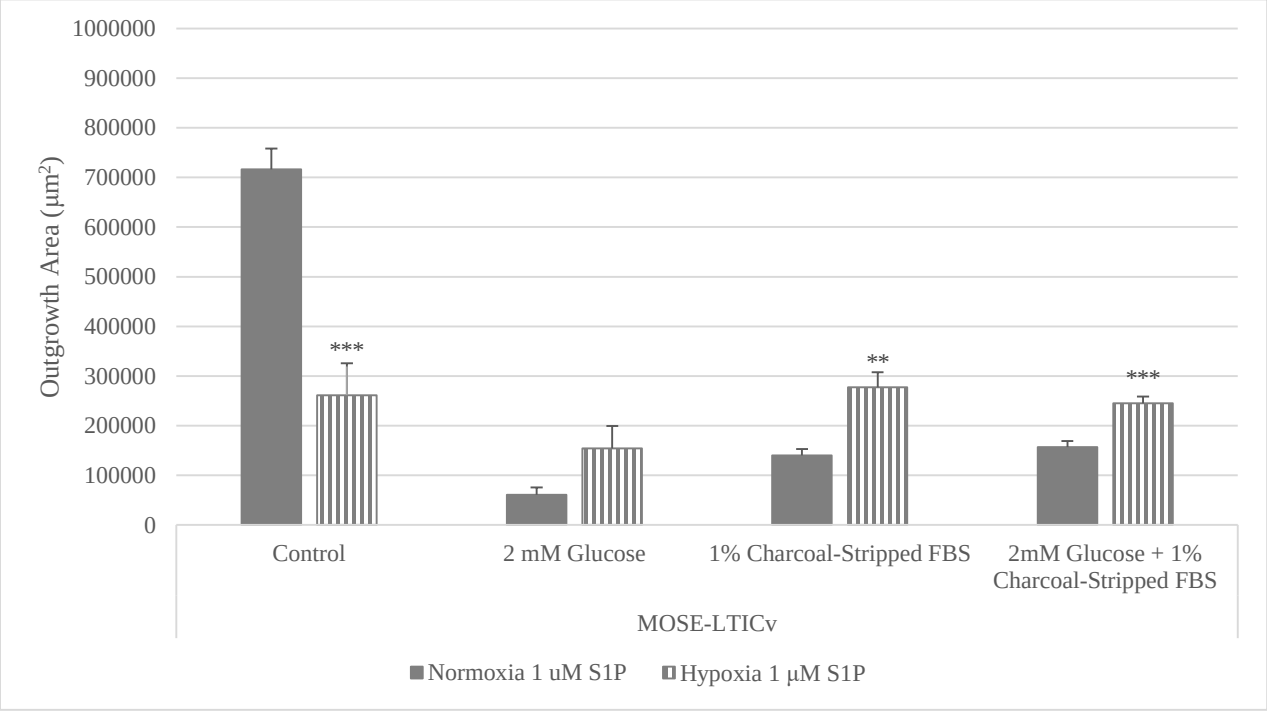

Figure 27. Comparison of S1P treatment on MOSE-LTICv spheroid outgrowth in hypoxia and normoxia. Significance was assessed using one-way ANOVA analysis (* indicates $p \leq 0.05$).

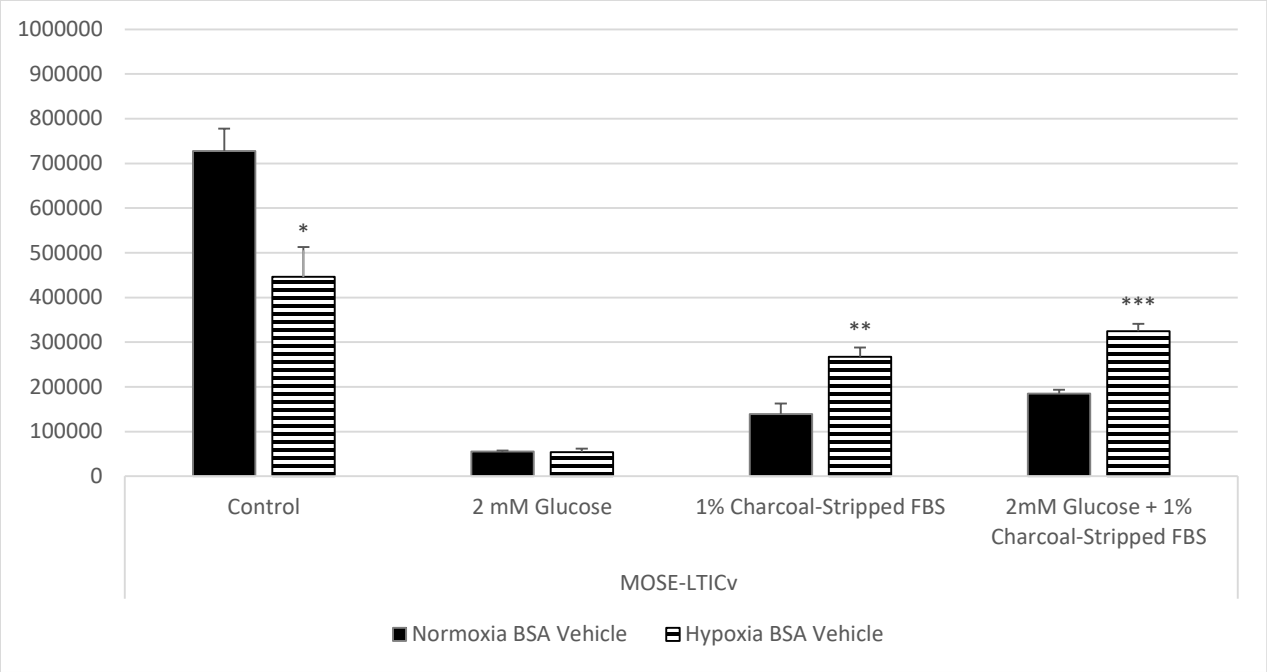

Figure 28. Comparison of BSA vehicle treatment on MOSE-L$_{TICv}$ spheroid outgrowth in hypoxia and normoxia. Significance was assessed using one-way ANOVA analysis (* indicates $p \leq 0.05$, ** indicates $p \leq 0.01$, *** indicates $p \leq 0.001$).

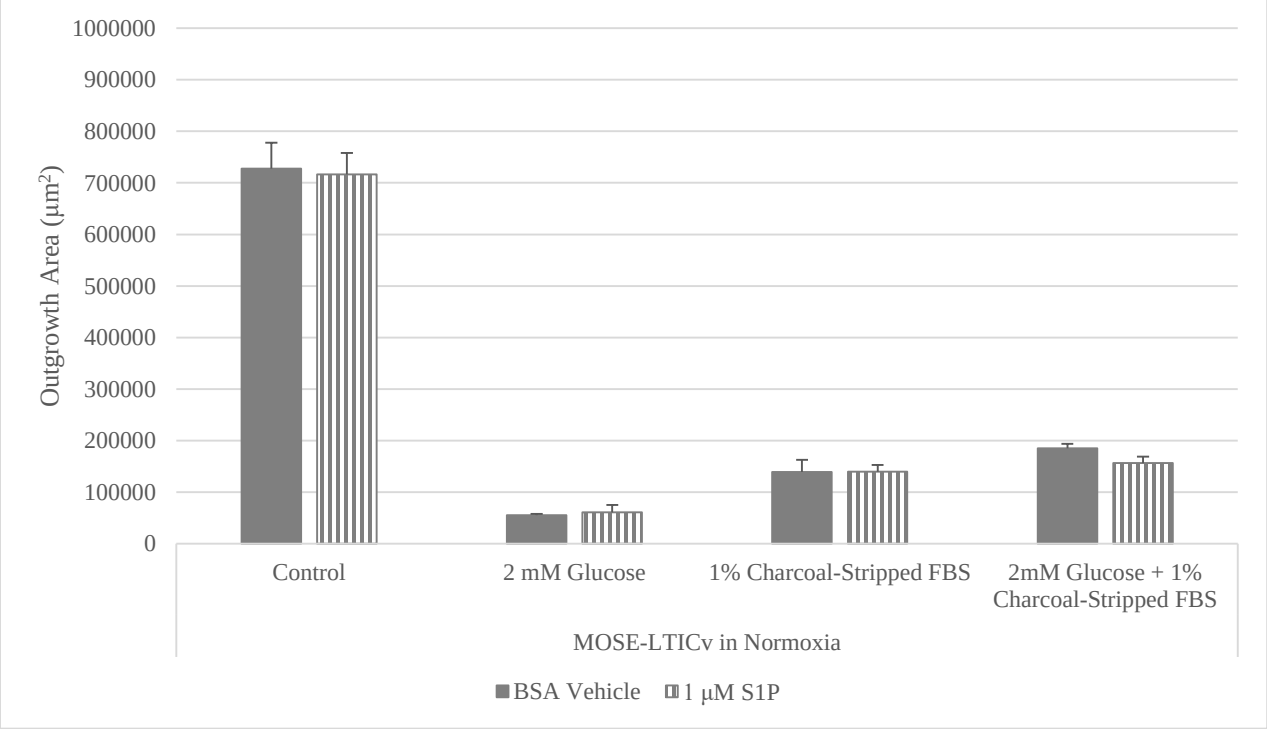

Figure 29. Effect of BSA vehicle or S1P treatment on MOSE-L$_{TICv}$ spheroid outgrowth in normoxia. Significance was assessed using one-way ANOVA analysis.

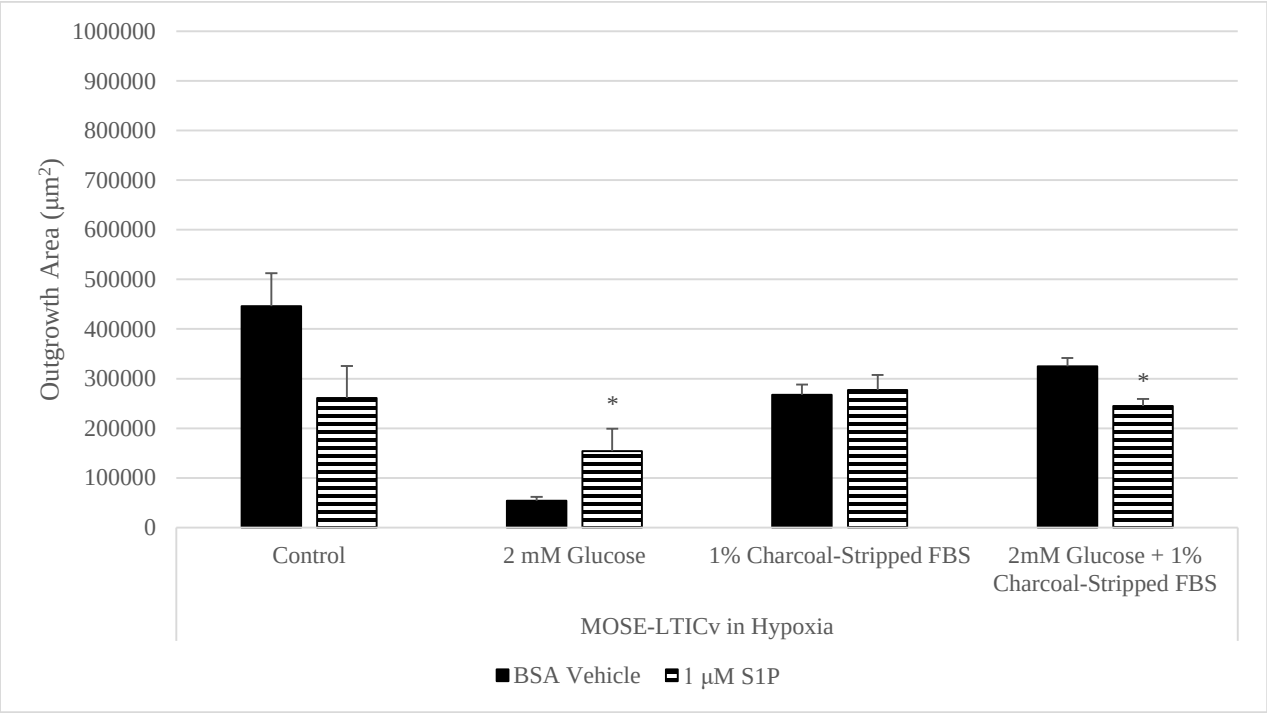

Figure 30. Effect of BSA vehicle or S1P treatment on MOSE-L_{TICv} spheroid outgrowth in hypoxia. Significance was assessed using one-way ANOVA analysis (* indicates $p \leq 0.05$).

S1P	Normoxia	Hypoxia
	MOSE-L_{TICv}	MOSE-L_{TICv}
Control Medium	▭	▭
LG Medium	▭	⇧
CS Medium	▭	▭
-CS -LG Medium	▭	⇩

Table 6. Summary of the impact of S1P on MOSE spheroid outgrowth when co-cultured under varying conditions using 24 hour measurements compared to controls. ⇧ = Increase in outgrowth, ⇩ = decrease, ▭ = no change.

MOSE-L Spheroids Interact with Stromal Cells but not S1P to Adhere in Nutrient-Starved Environments

While the MOSE-L_{TICv} spheroids readily adhere and outgrow regardless of stromal cell incorporation and nutrient-starved conditions, MOSE-L cells are less able to adapt and proliferate in nutrient-starved environments. The same experiment was performed as previously described. MOSE-L spheroids had measurable outgrowth in control medium; however, there was no measurable outgrowth in many of the nutrient-starved conditions. There were no observed differences between treatment groups (both S1P and SVF co-culturing) in control medium, which is inconsistent with our hypothesis. S1P and stromal cells thus do not play a role in increasing spheroid outgrowth in control medium for MOSE-L spheroids. Since there was no difference between S1P or SVF treatment, analysis turned to comparison between hypoxic and normoxic environments. The only significant difference between groups was the increased outgrowth area of the heterogeneous spheroids in hypoxia compared to normoxia (Fig. 31). Interestingly, however, a trend exists for the MOSE-L that is the opposite to the MOSE-L_{TICv}—a seemingly larger outgrowth area in hypoxia, though not significant in homogeneous samples (Fig. 31). Two replicates of the heterogeneous MOSE-L spheroids in hypoxia are depicted to visualize the significant difference in outgrowth area between hypoxia and normoxia (Fig. 32)—note the spheroid size difference and outgrowth area difference. These results build on previous findings that hypoxic responses can vary greatly compared to normoxic responses, highlighting the variability between these culture conditions and the importance of analyzing data in relevant conditions.

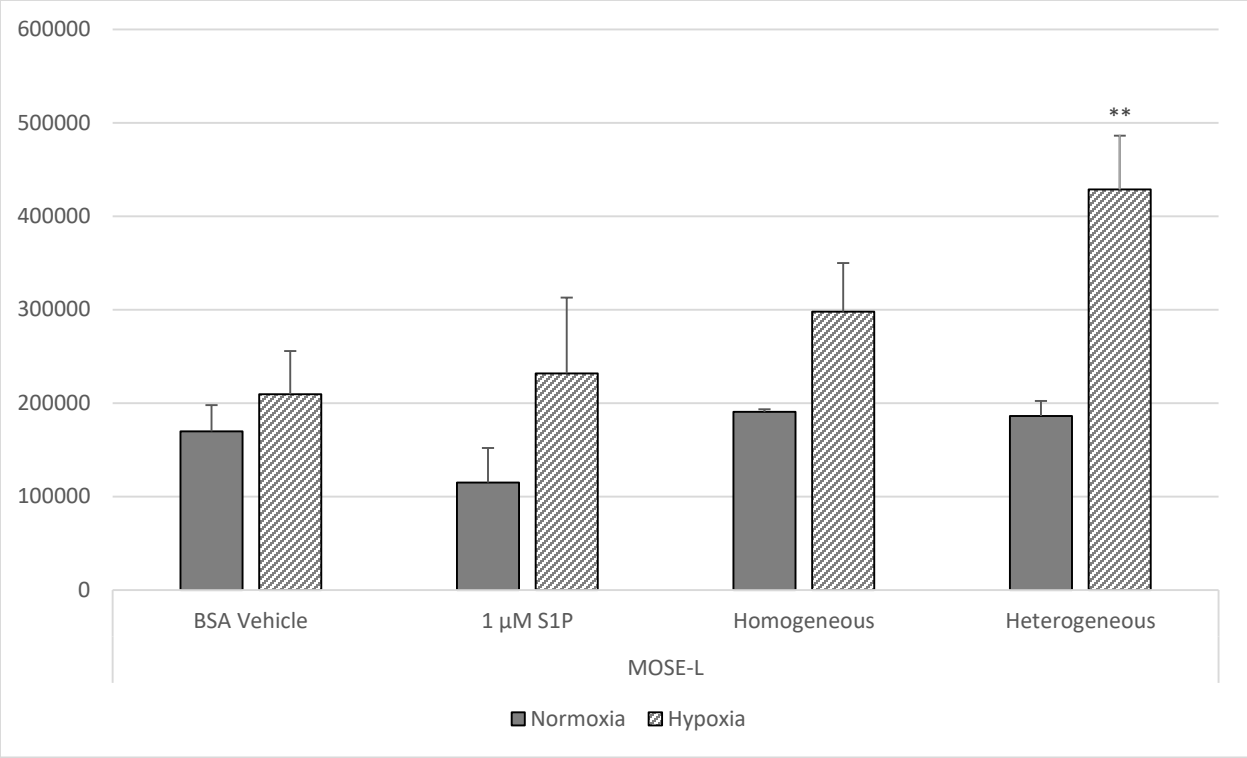

Figure 31. Comparison of outgrowth area of MOSE-L spheroid treatment groups in hypoxia and normoxia. Significance was assessed using one-way ANOVA analysis and correlates to respective treatment group in normoxia (** indicates $p \leq 0.01$).

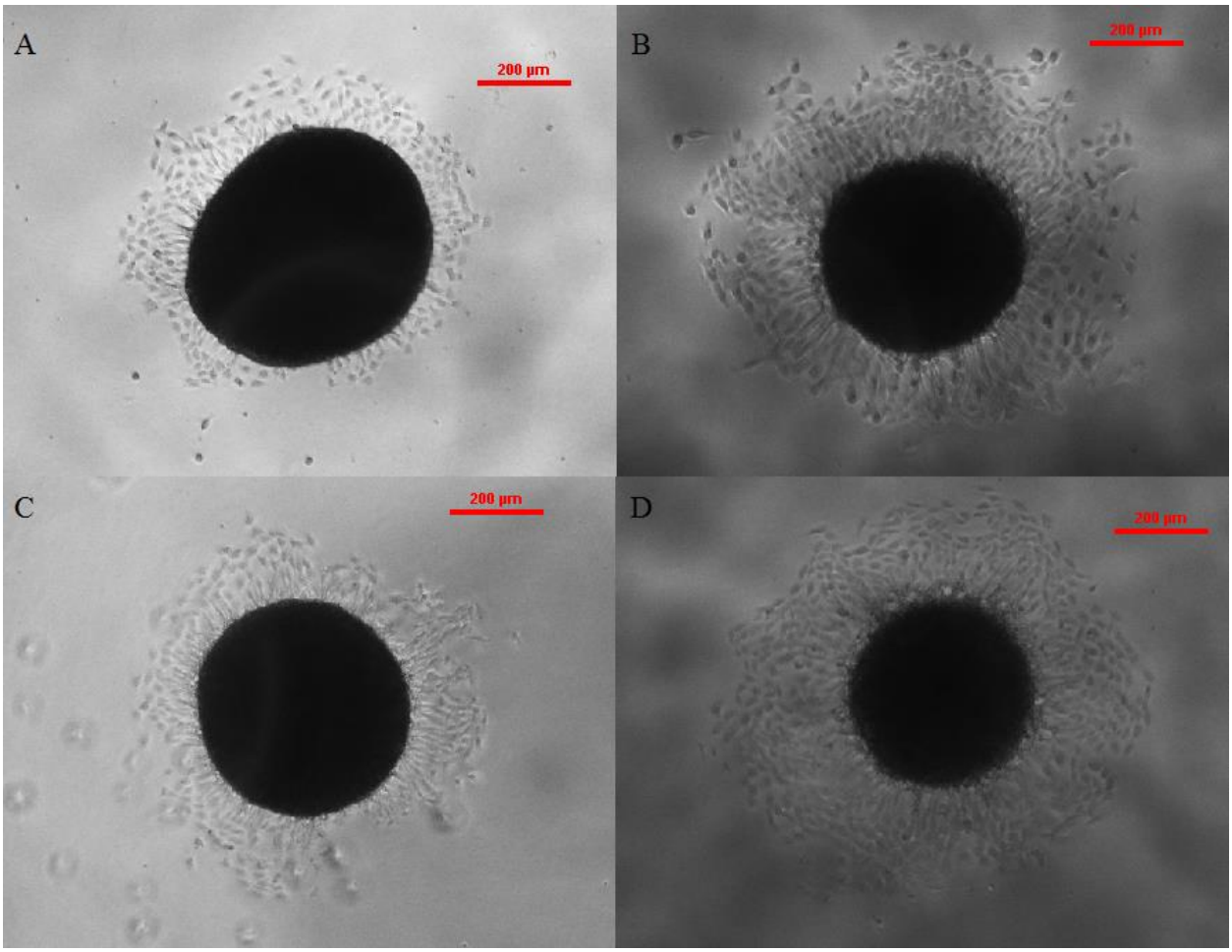

Figure 32. Two biological replicates of heterogeneous MOSE-L spheroids in normoxia (A, C) and hypoxia (B, D).

While there was not enough outgrowth in the MOSE-L spheroids for measurable analyses as in the MOSE-L_{TICv} spheroids, qualitative image analyses were performed to assess the importance of S1P and stromal cells in nutrient-starved conditions for MOSE-L spheroids. S1P appears not to play a critical role in MOSE-L spheroid adherence. In normoxia, 1 out of 5 spheroids adhered in 1 µM S1P LG medium compared to 0 out of 4 in BSA vehicle LG medium, 2 out of 6 adhered in the S1P CS medium compared to 3 out of 6 in the BSA vehicle CS medium, 4 out of 5 adhered in the S1P LG+CS medium compared to 6 out 6 adhering in the BSA vehicle LG+CS medium (Table 7). In hypoxia, none of the six spheroids adhered in either S1P or BSA LG medium, 4 out of 6 adhered in S1P CS medium compared to 4 out of 5 adhering in the BSA CS medium,

and all 6 spheroids adhered in both S1P and BSA LG+CS medium (Table 7). Thus, S1P may not play a role in aiding adhesion and outgrowth of MOSE-L spheroids. S1P thus neither plays a role in spheroid proliferation in physiologically relevant conditions nor in spheroid adhesion and outgrowth of MOSE-L cells.

	Normoxia			Hypoxia		
	2 mM Glucose	1% CS FBS	2 mM Glucose + 1% CS FBS	2 mM Glucose	1% CS FBS	2 mM Glucose + 1% CS FBS
BSA Vehicle	0/4	3/6	6/6	0/6	4/5	6/6
1 μM S1P	1/5	2/6	4/5	0/6	4/6	6/6

Table 7. Number of adhered MOSE-L spheroids out of total viable transferred spheroids in each condition.

The stromal cells appear to have a more potent effect on allowing MOSE-L spheroids to adhere in nutrient-sparse conditions. In each treatment (LG, CS, LG+CS), the inclusion of stromal cells in the cancer spheroids increased the number of spheroids from the two MOSE-L replicates that adhered (Table 8). In normoxia, the stromal cells were rather effective in facilitating adherence of MOSE-L spheroids that did not adhere in homogeneous conditions. This effect was stronger in hypoxia, in which 100% of the MOSE-L spheroids adhered to the respective medium treatment with stromal cell addition compared to homogeneous replicates (Table 8). An image of two replicates of MOSE-L homogeneous, unattached spheroids in LG medium in both hypoxia and normoxia compared to their heterogeneous counterparts with visible outgrowth highlights the ability of the stromal cells to allow these spheroids to adapt to LG medium conditions (Fig. 33). A similar image is shown for CS medium (Fig. 34). These results suggest that stromal cells aid in the adhesion of MOSE-L spheroids, even in nutrient-starved, hypoxic conditions that are not

permissive for adherence. Stromal cells—and perhaps not S1P—may play a role in MOSE-L spheroid adhesion.

	Normoxia			Hypoxia		
	2 mM Glucose	1% CS FBS	2 mM Glucose + 1% CS FBS	2 mM Glucose	1% CS FBS	2 mM Glucose + 1% CS FBS
Homogeneous MOSE-L	0/3	0/4	2/4	0/4	2/4	2/3
Heterogeneous MOSE-L	3/4	2/4	4/4	4/4	4/4	4/4

Table 8. Number of adhered MOSE-L homogeneous and heterogeneous spheroids out of total viable transferred spheroids in each condition. This experiment used two biological replicates instead of three.

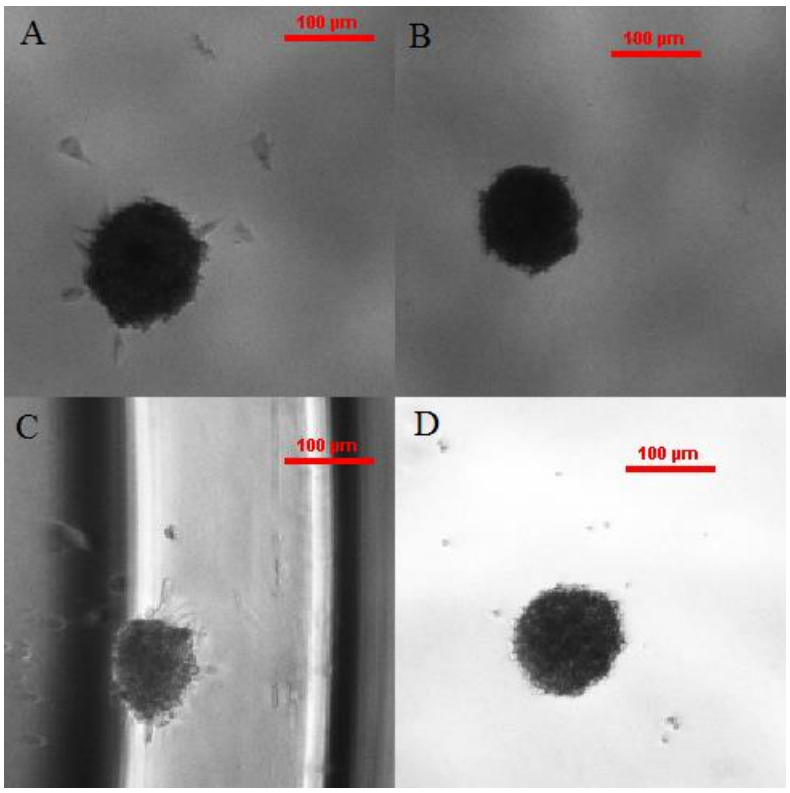

Figure 33. Two replicates of homogeneous (B, D) and heterogeneous (A, C) MOSE-L spheroids in LG medium in hypoxia (A, B) and normoxia (C, D). A and C have clear attachments to the plate, while B and D do not.

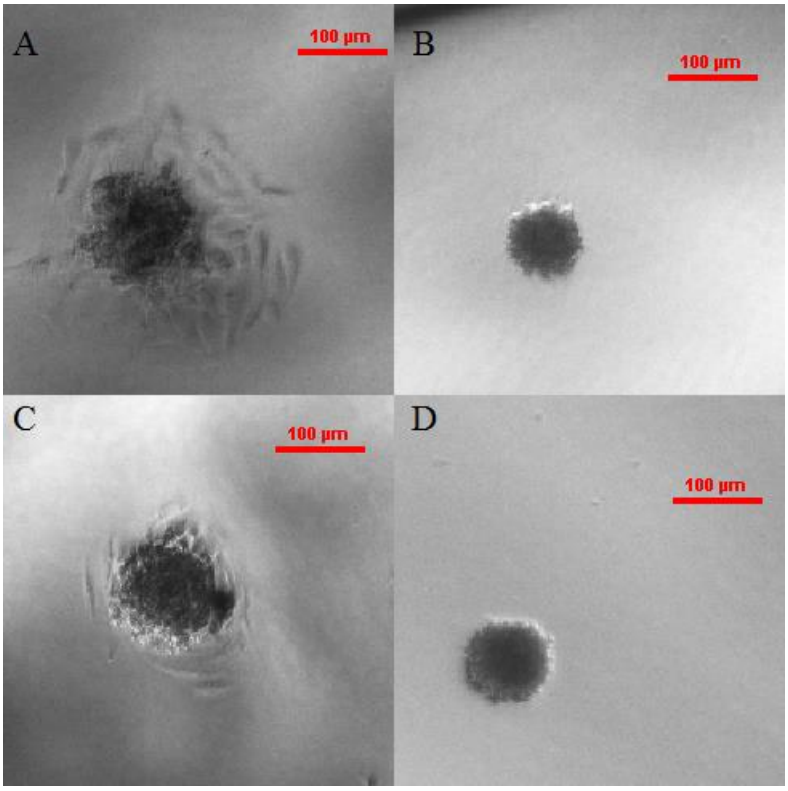

Figure 34. Two replicates of homogeneous (B, D) and heterogeneous (A, C) MOSE-L spheroids in hypoxia (A, B) and normoxia (C, D) in 1% CS FBS medium. A and C have extensive outgrowth on the plate, whereas B and D have no visible attachment.

The mechanism how the stromal cells can facilitate the MOSE-L cancer spheroids adherence in nutrient-starved environments remains to be elucidated. The stromal cells do, however, have an ability to adhere and grow in these harsh conditions by themselves after the same treatment as the cancer cells (5 days as a spheroid → tissue-cultured plate). In fact, all of the transferred stromal cell spheroids adhered to each of the conditions with the exception of the LG medium in normoxia (Table 9). The origin of these cells, the hypoxic obese adipose tissue, may contribute to this effect. The adherence and outgrowth of the stromal cells in these conditions is shown below (Fig. 35).

	Normoxia			Hypoxia		
	2 mM Glucose	**1% CS FBS**	**2 mM Glucose + 1% CS FBS**	**2 mM Glucose**	**1% CS FBS**	**2 mM Glucose + 1% CS FBS**
Homogeneous SVF	**0/3**	**3/3**	**3/3**	**3/3**	**3/3**	**3/3**

Table 9. Number of adherent SVF spheroids in each of the nutrient-starved conditions.

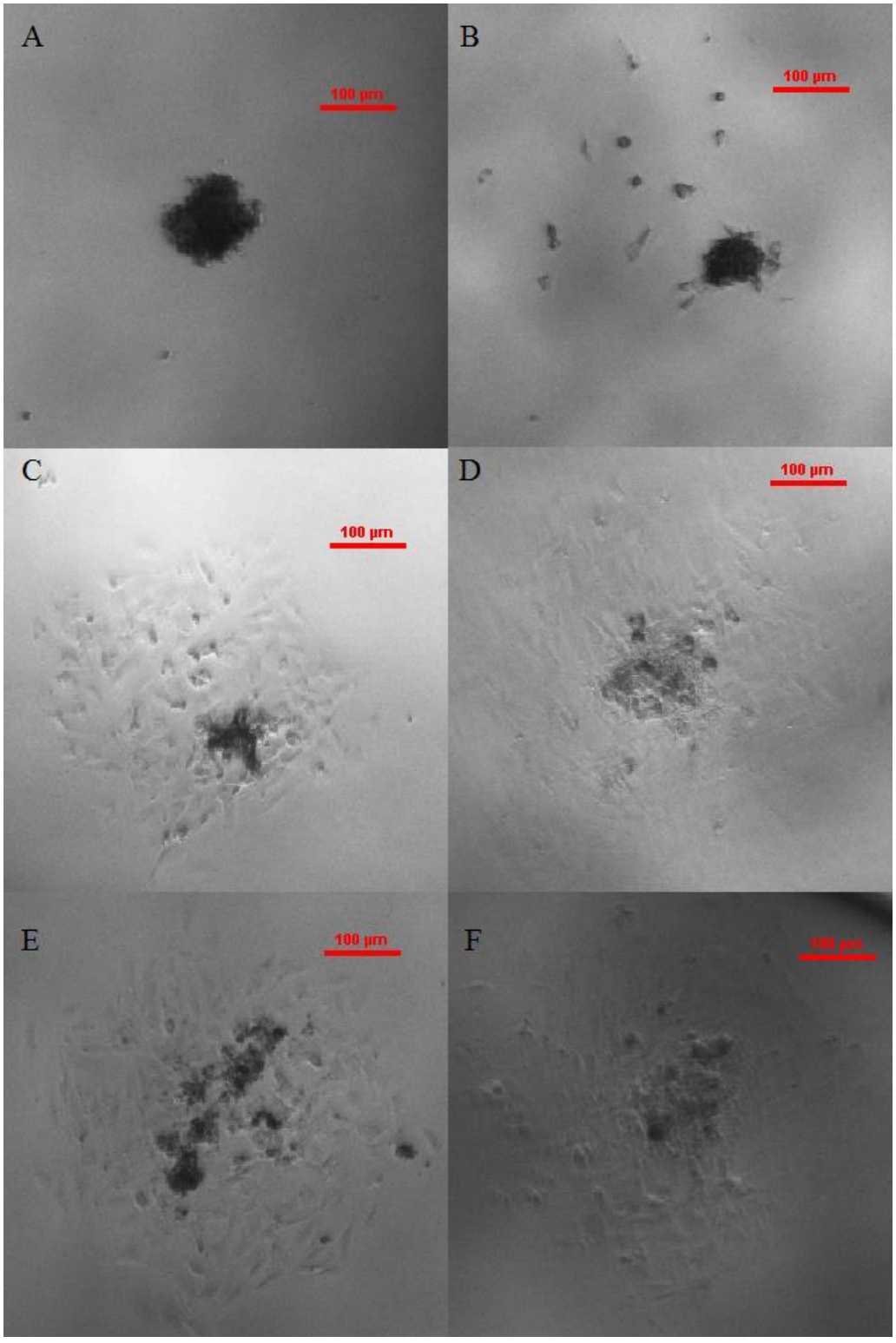

Figure 35. Adherence and outgrowth of SVF spheroids in normoxia (left three images) and hypoxia (right three images). Treatments are LG medium (A and B), CS medium (C and D), and LG+CS medium (E and F). Outgrowth is visible in all groups except normoxia LG (A).

To assess if the outgrowths in the heterogeneous spheroids were cancer cells or the stromal cells due to their inherent ability to adhere to these conditions more efficiently than the MOSE-L spheroids, cell tracker was added to the SVF cells in heterogeneous spheroid formation and the spheroids were then transferred to a tissue-cultured plate. Under normoxic conditions, we sampled heterogeneous spheroids that adhered in all medium conditions (control, LG, CS, LG+CS). Cell tracker revealed that the bulk of the stromal cells are maintained in the core of the spheroid, even after the spheroid adheres and there is visible outgrowth (Fig. 36). While the stromal cells may play a role in helping the cancer spheroids adhere, it is suggested that the outgrowth consists primarily of cancer cells. While we have previously shown the 3D association between MOSE and SVF cells (Fig. 9), our preliminary data here suggests that there is not strong 2D association of these cells—it appears that stromal cells are not needed for spheroid outgrowth in 2D conditions.

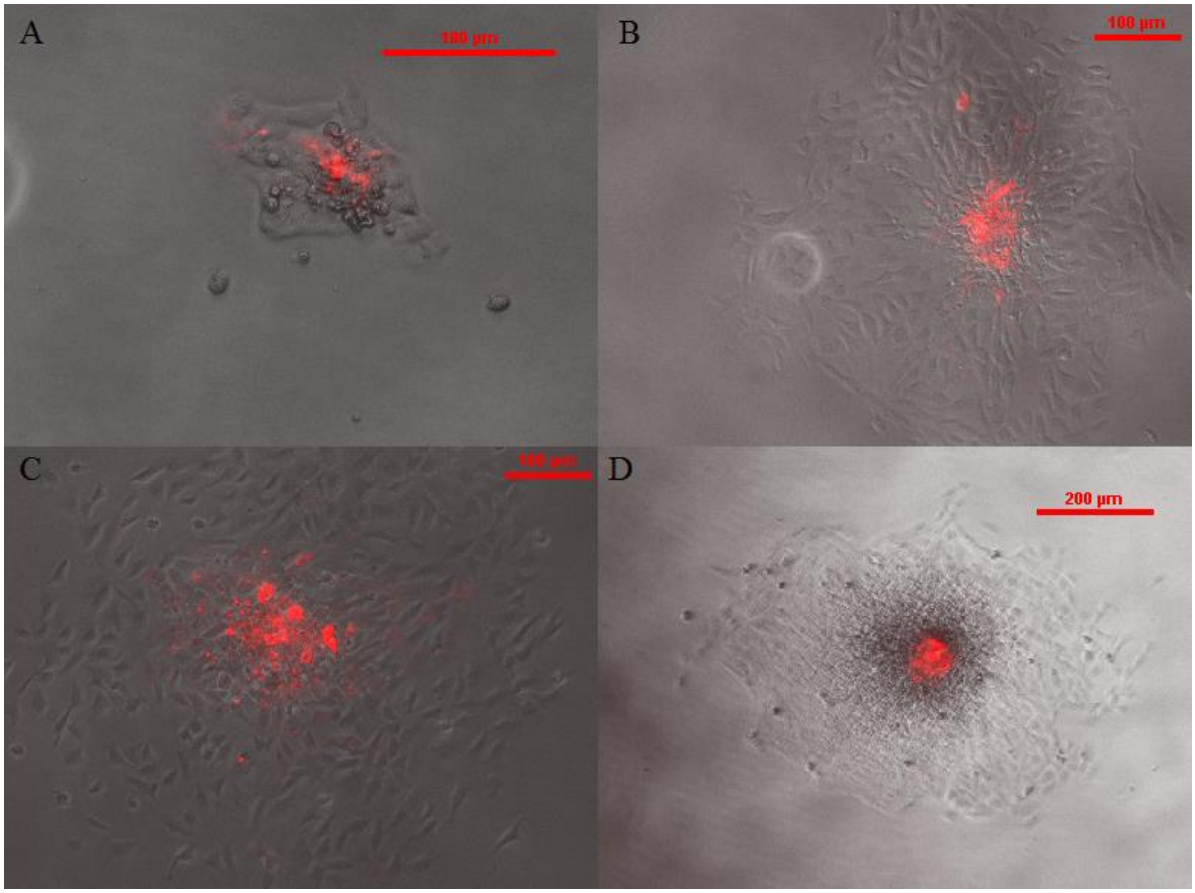

Figure 36. Merged images of adhered heterogeneous spheroids with stromal cells (red) and MOSE-L cells (brightfield) in varying medium conditions in normoxia. (A) LG medium, (B), CS medium, (C) LG+CS medium, (D) control medium.

S1P and Stromal Cells May Facilitate Aggressive Invasion

To test the effectiveness of S1P and stromal cells in inducing an aggressive and invasive phenotype, homogeneous spheroids with BSA vehicle or 1 µM S1P treatment and heterogeneous spheroids with stromal cells were treated with the four medium conditions and implanted in collagen under normoxia. Images were taken at 24 hours to qualify invasive phenotypes. Images taken seem to suggest that both S1P and stromal cells contribute to an aggressive phenotype in certain treatments of MOSE-L and MOSE-L_{TICv} spheroids (Figs. 37-40). A marker of efficient invasion is strong, thick protrusions as opposed to smaller, more widespread invasions into the matrix. Both S1P and stromal cells appear to increase the invasive capacity of both MOSE-L and

MOSE-L_{TICv} spheroids under varying conditions. These results are consistent with our hypothesis that S1P and stromal cells are a mediator of an aggressive invasive phenotype. While many of our previous results do not see a significant increase in spheroid size and outgrowth with S1P and SVF treatment in physiologically relevant conditions, it appears that S1P and SVF cells increase the number of invasive protrusions generated in MOSE spheroids. The mechanisms behind this remain to be elucidated.

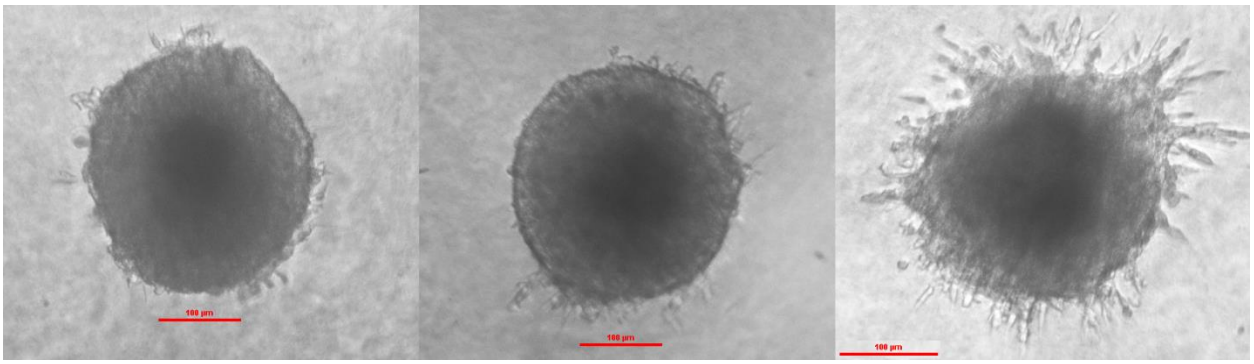

Figure 37. Invasion of MOSE-L_{TICv} spheroids in CS medium with (A) BSA Vehicle (B) 1 μM S1P (C) Heterogeneous SVF

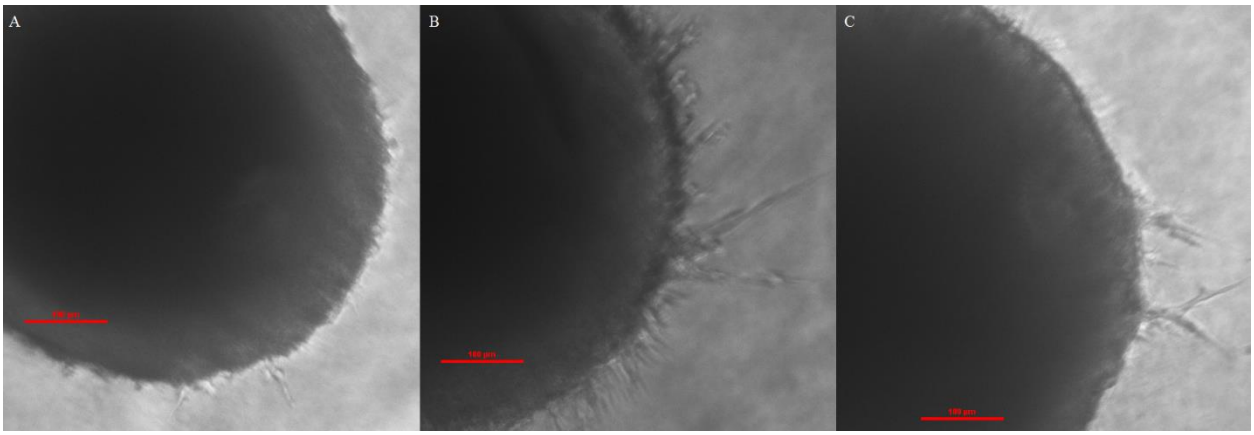

Figure 38. Invasion of MOSE-L_{TICv} spheroids in control medium with (A) BSA Vehicle (B) 1 μM S1P (C) Heterogeneous SVF

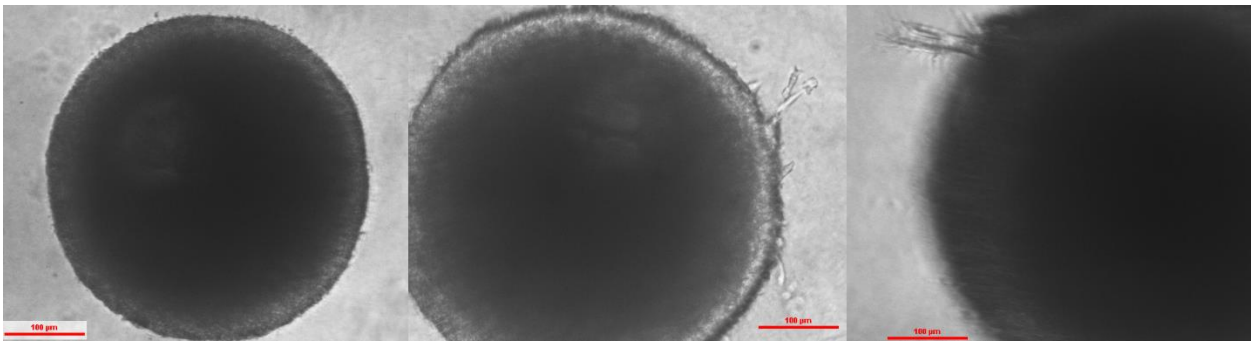

Figure 39. Invasion of MOSE-L spheroids in control medium with (A) BSA Vehicle (B) 1 μM S1P (C) Heterogeneous SVF

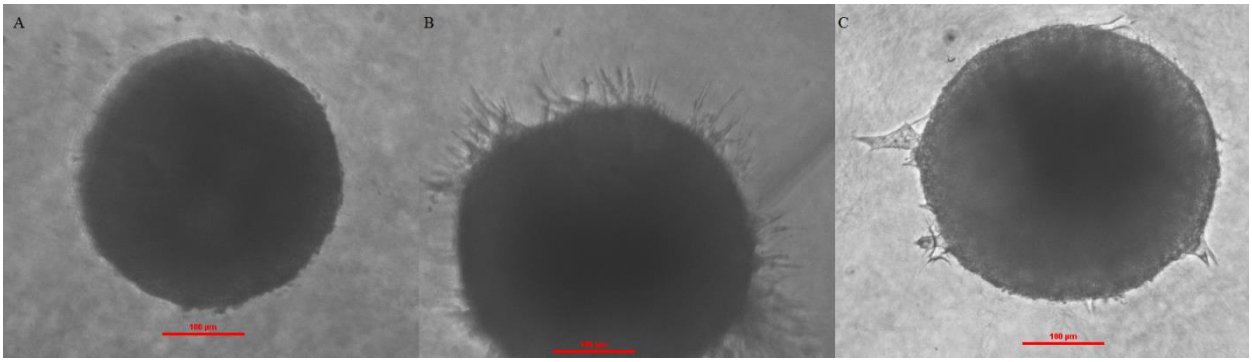

Figure 40. Invasion of MOSE-L spheroids in LG medium (A and B) or LG+CS medium (C) with (A) BSA vehicle (B) Heterogeneous SVF (C) Heterogeneous SVF

Sphingosine Kinase Inhibitor

To test the effectiveness of a SphK1 inhibitor, an MTT assay was performed on malignant cells after exposure to the inhibitor in varying concentrations for 72 hours. The MOSE-L and MOSE-L_{TICv} cells exhibited toxic effects of the inhibitor around a 2.5 μM dose, with almost no cell signal at 10 μM (Fig. 41). These results indicate that a SphK1 inhibitor can reduce cell proliferation of malignant MOSE cells, as we hypothesized due to the reliance of S1P by these cells. As expected, the highly malignant tumor-initiating cells respond more strongly than the late stage cells at lower concentrations of the inhibitor (0.5 μM), indicating their reliance on this compound for proliferation. Moreover, lower concentrations of this inhibitor could be useful in potentially attenuating other metastatic implications of S1P, such as invasion.

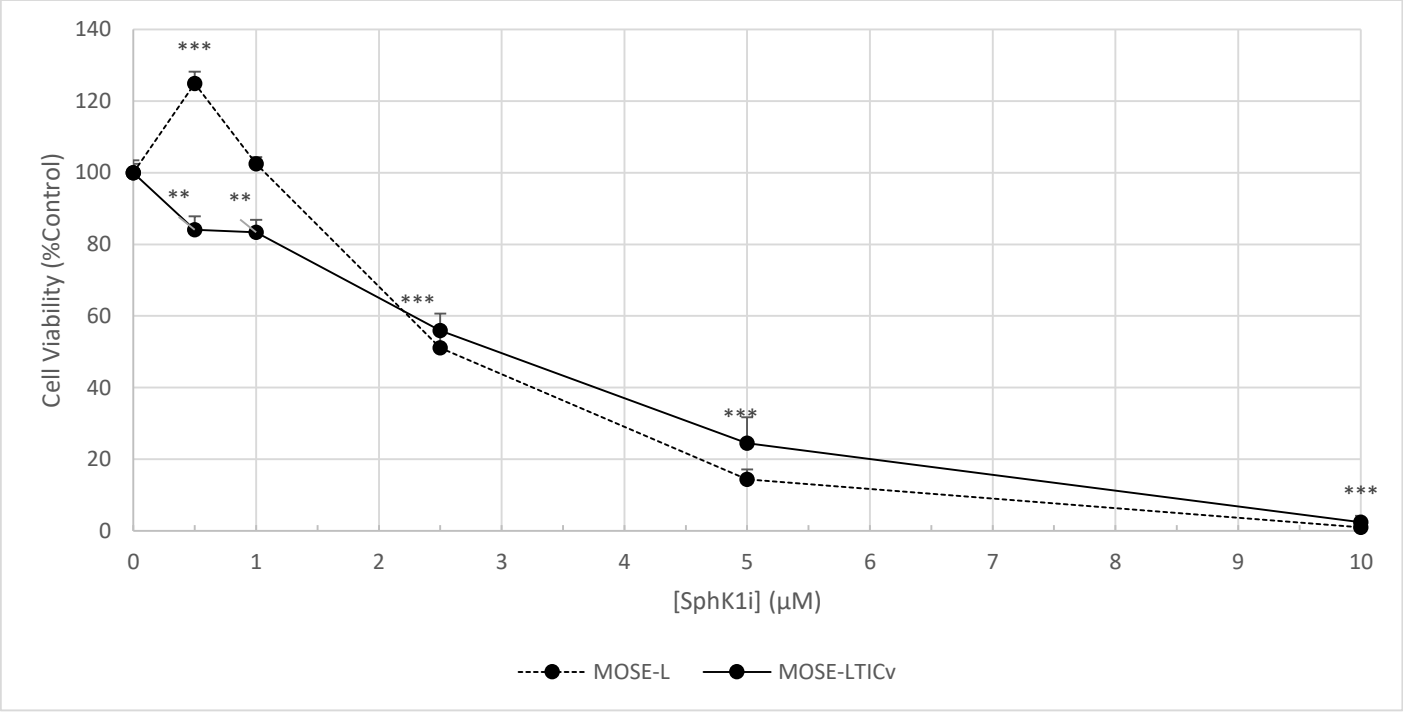

Figure 41. MTT assay of monolayer MOSE-L and MOSE-L_{TICv} cells in control medium with SphK1 treatment. Viability was standardized as the percentage of the respective cell type control with maximum DMSO vehicle treatment at 10 μM in normoxia. Significance was assessed using one-way ANOVA analysis (** indicates $p \leq 0.01$, *** indicates $p \leq 0.001$). MOSE-L_{TICv} utilized two biological replicates instead of three.

V. DISCUSSION

The intrinsically complex nature of ovarian cancer metastasis tied with a research field inundated with experimental set-ups and analyses that are not physiologically relevant leaves a wide gap of knowledge that must be filled to first, understand the mechanisms of the disease and consequently second, develop better screening methods and therapeutic tools to prevent and treat this disease. The aim of this study is to elucidate some of the mechanisms behind which S1P and/or adipose-derived stromal cells may contribute to an aggressive phenotype of ovarian cancer. The aim was to identify a link between S1P and SVF cells in increasing the malignant profile of ovarian cancer as the disease progresses from primary site to metastasis elsewhere in the peritoneal cavity. Our experimental setup appropriately mimics the progression of the disease from an adherent monolayer to spheroid formation in the peritoneal cavity and subsequent

metastatic adhesion and invasion. These two treatment groups were designed to see if any upregulation of proliferation, outgrowth, or invasion was a response to S1P itself or if the stromal cells contributed to these factors via other mechanisms. While preliminary, the results indicate that these two factors may play a critical role in the development of a malignant, metastatic disease. However, in many regards, the results were not as robust as we initially hypothesized.

Sphingosine-1-Phosphate

S1P has yet to be well understood in the scope of ovarian cancer; however, the results of this study indicate a few critical contributions of this signaling molecule. First, S1P contributes significantly to a more proliferative phenotype of adherent, malignant ovarian cancer cells. One of the first stages of cancer development is the rapid proliferation of the primary site cells—although MOSE-L variants are likely already exfoliated, particularly the tumor initiating cell variants. Exposure to high levels of S1P may thus be a critical part of the beginning stages of aggressive ovarian cancer progression. Second, S1P may promote the generation of invasive structures. While collagen invasion assays are qualitative and rather difficult to draw concrete conclusions from, it appears that S1P may promote the formation of invasive structures into extracellular matrices to develop a highly aggressive and metastatic disease. The mechanism behind this apparent upregulation of invasive structure generation remains to be elucidated quantitatively, via gene expression and/or protein upregulation of invasive markers. However, this is difficult with the lack of well-established markers of invasion in ovarian cancer. This paper moreover introduces the idea of a SphK1 inhibitor to target over-proliferative malignant cancer cells as potential therapeutic agent. While this is preliminary, it is an interesting starting point for more research to potentially prevent the metastatic actions of S1P. Moreover, this

inhibitor could be used to attenuate its potential promotion of an invasive profile. However, if this inhibitor aims to target S1P from stromal cells via their intrinsically high SphK1 levels to cancer spheroids and tumors, a few experimental setbacks arise. First, co-culturing heterogeneous spheroids with the inhibitor may not give an accurate picture of the SVF contribution since the MOSE cells would also be cultured with the inhibitor. Second, if culturing SVF cells with the inhibitor initially and then co-culturing them with MOSE cells in a spheroid, the long-term effectiveness of the inhibitor would need to be assessed upon incorporation of the SVF cells in a MOSE spheroid in inhibitor-free medium. Nevertheless, this inhibitor is introduced as a potential treatment in ameliorating some of the aggressive profile from S1P, perhaps secreted from the stromal cells—and in other aggressive contributions that were not assessed in this study.

At the same time, many questions must be discussed about some findings of S1P in this study. First, our hypotheses about S1P were overstated. While S1P may be implicated in adherent monolayer growth and invasive structure generation, it is unclear if it contributes to a more proliferative 3D spheroid. Our experiments indicated an increase in spheroid size in MOSE-L spheroids with S1P treatment in control medium, although the relevancy of a nutrient-rich condition should be taken into consideration. However, caution must be taken in analyzing spheroid size as an indicator of cell proliferation. It is difficult to tell how compact and proliferative a spheroid might be beyond its surface area. We have noted some spheroids with objectively larger sizes having much more debris than smaller spheroids. This debris indicates a higher number of unviable, sloughed cells exfoliated from the spheroid—would more debris indicate an unhealthy spheroid (Fig. 42)? These are important things to consider when using size as a measurement of spheroid viability. The difficulty in using viability assays on spheroids this

size limits potential answers to this question. For now, it is unclear if spheroid size correlates to spheroid proliferation; thus, it is unclear what role S1P might play when the cancer cells form a 3D structure. Nevertheless, our size data may suggest its proliferative role in control conditions. However, in contrast to what we initially hypothesized, S1P did not increase spheroid size in the nutrient-starved, physiologically relevant conditions—whether in hypoxia or normoxia. We conclude that S1P upregulates malignant MOSE proliferation in the control medium monolayer; however, S1P does not rescue the malignant MOSE spheroids in starved medium conditions. S1P is thus tentatively not implicated as a factor in spheroid proliferation under physiologically relevant conditions.

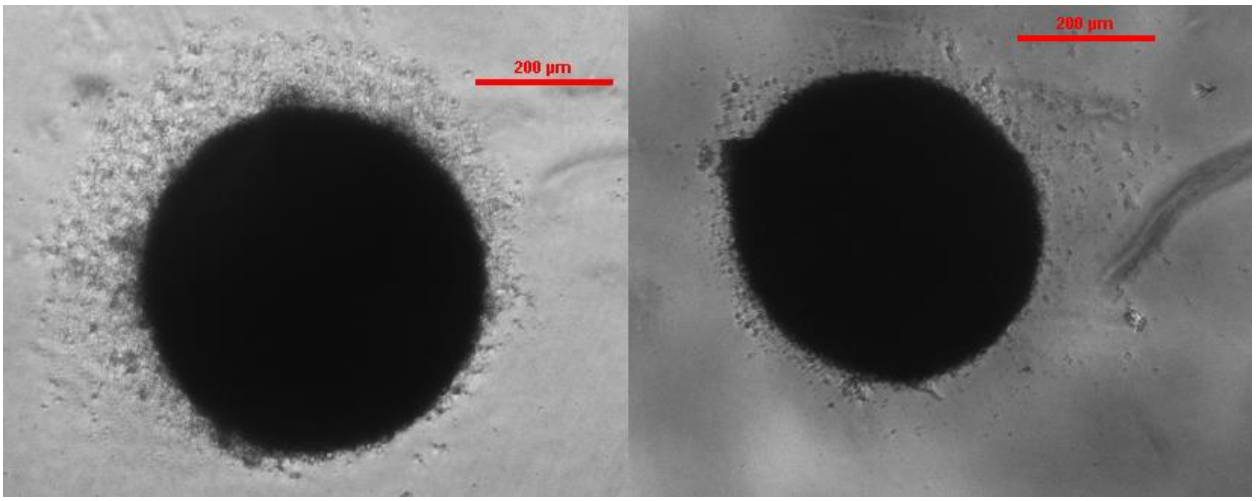

Figure 42. Image of a S1P-treated spheroid (left) and a BSA vehicle-treated spheroid. The left spheroid was calculated to be 39171 μm^2 larger than the right spheroid; however, it has much more debris.

Outgrowth is another tool that might be useful in determining cell viability. As previously shown in Fig. 32, a large spheroid size might not necessarily correlate with a large, adherent outgrowth. However, outgrowth might be a similarly complex tool to assess viability. If a spheroid requires MET to successfully adhere to a surface, does it require losing some of its identity as a spheroid for proper adhesion? It is further complicated by the types of outgrowths

observed. Some spheroids appear to have a “flatter” phenotype upon adhering and then have a seemingly disorganized outgrowth. Others maintain their spheroid core and have a nice plush, organized outgrowth (Fig. 43). It is difficult to tell which is more “viable” beyond a simple measurement of outgrowth area, although it is certainly a productive place to start. Regardless, we did not observe a marked difference in MOSE-L_{TICv} spheroid outgrowth area with S1P treatment or SVF incorporation in many of our experimental conditions; however, we did see an increase in outgrowth size in LG medium in hypoxia under both treatment groups. While this increased outgrowth is apparent in one of our more relevant culture conditions (LG hypoxia), the overall impact of S1P and SVF cells on spheroid outgrowth were overstated in our hypothesis. It appears that S1P and SVF cells may not be implicated in spheroid outgrowth, although there is some evidence that it might play a role under certain conditions.

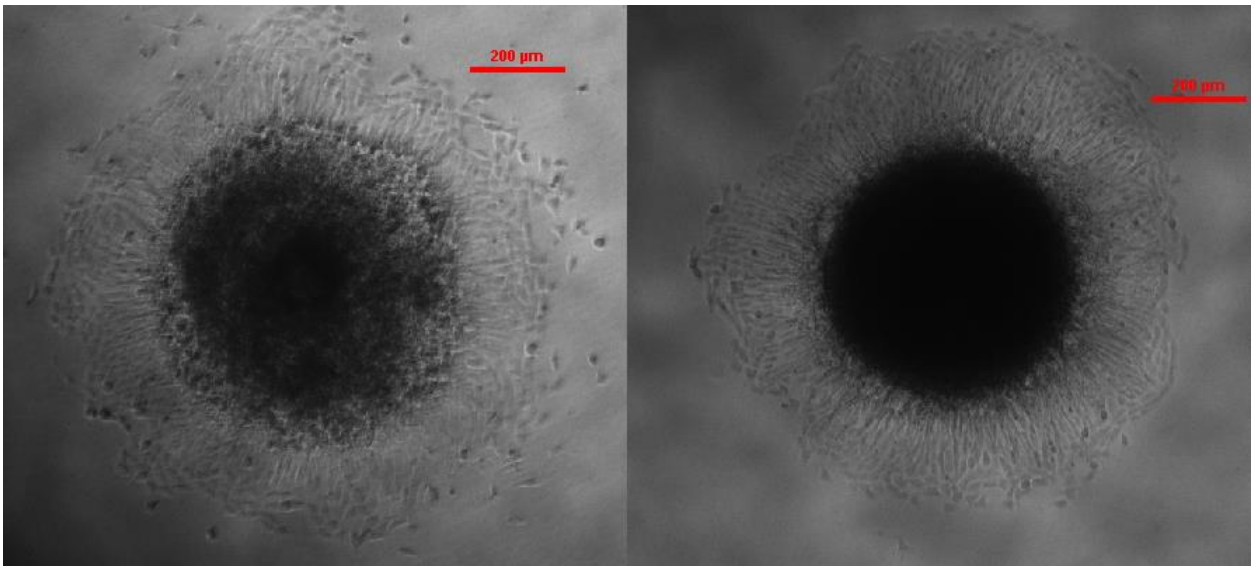

Figure 43. MOSE-L_{TICv} spheroid outgrowth phenotypes. Left spheroid with a more flattened phenotype and somewhat disorganized outgrowth. Right spheroid with an in-tact spheroid core and plush outgrowth.

Stromal Cells

This study indicates that stromal cells do not necessarily protect cancer cells or promote survival in nutrient-starved medium conditions by size measurement—although they do increase spheroid size in control medium. They do, however, play a critical role in aiding adhesion of MOSE-L cancer spheroids and by enhancing invasive properties of heterogeneous MOSE-L spheroids. We have previously shown the ability for heterogeneous cancer spheroids to recruit stromal cells in their invasive structures;[38] the prominent protrusions in the invasion assay from heterogeneous spheroids has clear implications for the metastatic potential of the attached spheroids. However, it appears as if their 2D association may be less relevant in spheroid outgrowth, as indicated in the cell tracker experiment showing the centralization of SVF cells in the center of the spheroid (Fig. 36). Furthermore, despite a rather small sample size and a qualitative analysis, the ability for stromal cells to adhere cancer spheroids is rather clear—homogeneous replicate counterparts do not adhere but heterogeneous ones do. This warrants further investigation into the mechanisms by which stromal cells might promote spheroid adhesion, perhaps via upregulation of certain adhesion proteins within the spheroid, although this faces similar problems as examining candidate markers for adhesion—there is a lack of well-established markers for ovarian cancer spheroid adhesion. Moreover, the observation that heterogeneous—and to a lesser extent, homogeneous—spheroids also have the ability to adhere to ultra-low adherence plates in certain medium conditions is a fascinating prospect that warrants further investigation. This study establishes stromal cells as a contributor to a metastatic ovarian cancer disease state and necessitates further research into the mechanisms behind these observations and the variations in stromal cell populations that might alter these effects. Nevertheless, our hypothesis was still overstated. Stromal cells do not contribute as strongly as we initially anticipated to ovarian cancer aggressiveness. We expected them to significantly rescue

spheroids in nutrient-starved conditions, which was not observed. Furthermore, stromal cells appear to have little effect on the MOSE-L_{TICv} spheroid outgrowth; however, there was an increased outgrowth in hypoxia with LG medium. This study elucidates that stromal cells may not be implicated in spheroid proliferation and outgrowth of late-stage, aggressive spheroids; rather, they may play a key role in adhesion and invasion of ovarian cancer spheroids.

Hypoxia & Physiologically Relevant Conditions

Perhaps the most critical piece of this study is the experimental conditions and readouts. Some important results of this study stem from using physiologically relevant conditions. S1P-induced adherent proliferation is more robust for MOSE-Ls in hypoxia (Figs. 10 and 11). Furthermore, the ability for stromal cells to adhere most efficiently in relevant conditions both independently and as a part of heterogeneous cancer spheroid is integral to the context of ovarian cancer progression and future research in this field (Figs 33, 34, and 35). These results highlight the need to conduct future studies in relevant culture conditions—hypoxia—and utilizing nutrient conditions that appropriately mimic the environment the cancer cells are exposed to. We see an increase in spheroid size with S1P supplementation and stromal cell integration in MOSE-L cells; however, we do not see the similar crossover into nutrient-starved conditions. Further studies should aim to use physiologically relevant conditions to produce results that actually mean something in the context of the disease. The various significant differences we see when comparing normoxic and hypoxic conditions highlight the variability of these spheroids under these conditions and suggest that a normoxic, nutrient-rich condition might not be the most accurate reflection of how ovarian cancer cells respond. However, one problem is defining what a "physiologically relevant" condition is. We experimented with several different setups to mimic the peritoneal cavity as a hypoxic, nutrient-starved condition; however, it is difficult to conclude

if any of our used conditions accurately reflect the peritoneal cavity. Data exists for the glucose levels in the peritoneal cavity of patients with bacterial peritonitis;[29] however, whether these readouts accurately reflect the same levels of ascites in women with ovarian cancer remains to be concluded, and our glucose levels used were lower than these findings. Furthermore, the variability across different patients poses another problem—it is difficult to have a relevant culture condition when the disease varies greatly among patients and the peritoneal environment is likewise variable.

VI. CONCLUSION

Overall, we show that S1P and stromal cells do not contribute strongly to the metastatic profile of ovarian cancer in every stage of the disease, from adherent monolayer to rapid metastasis. However, we demonstrate the ability for the both S1P and SVF to elicit a critical increase in invasive capacity. Furthermore, we suggest a potential role of SVF cells and S1P in promoting 3D MOSE-L spheroid proliferation in control medium, although this requires further analysis and more critical approaches. We did not see similar results in nutrient-starved conditions, indicating that stromal cells and S1P cannot rescue MOSE cells in these conditions. Moreover, adipose-derived stromal cells may play a critical role in improving adhesive properties of cancer spheroids, perhaps enhancing their MET and improving metastatic potential. Moreover, we highlight the importance of utilizing physiologically relevant conditions in hypoxic environments mimicking those in the peritoneal cavity to yield more relevant and conclusive results applicable to understanding and eventually preventing ovarian cancer metastasis. These observations require further investigation into molecular markers of adhesion and invasion to better elucidate the roles of S1P and stromal cells in contributing to an aggressive ovarian cancer phenotype. Our results suggest that further S1P and stromal cell analyses focus on different metastatic factors other than spheroid proliferation and spheroid outgrowth, since they were not implicated in experimental

analyses focused on these measurements. Further research into other aspects of a metastatic disease may reveal the contribution of these two factors in an aggressive ovarian cancer disease to potentially be targets for screening and treatment to improve the outcome of patients diagnosed with ovarian cancer.

References

1. United States Cancer Statistics: 1999–2013 Incidence and Mortality Web-based Report. Available from URL: www.cdc.gov/uscs.
2. Cancer Stat Facts: Ovarian Cancer. Available from URL: https://seer.cancer.gov/statfacts/html/ovary.html 2017].
3. Roberts PC, Mottillo EP, Baxa AC, et al. Sequential molecular and cellular events during neoplastic progression: A mouse syngeneic ovarian cancer model. NEOPLASIA. 2005;7: 944-956.
4. Kim RH, Takabe K, Milstien S, Spiegel S. Export and functions of sphingosine-1-phosphate. BBA - Molecular and Cell Biology of Lipids. 2009;1791: 692-696.
5. Mizugishi K, Yamashita T, Olivera A, Miller GF, Spiegel S, Proia RL. Essential Role for Sphingosine Kinases in Neural and Vascular Development. Molecular and Cellular Biology. 2005;25: 11113-11121.
6. Milstien S, Spiegel S. Sphingosine-1-phosphate: an enigmatic signalling lipid. Nature Reviews Molecular Cell Biology. 2003;4: 397-407.
7. Pralhada Rao R, Vaidyanathan N, Rengasamy M, Mammen Oommen A, Somaiya N, Jagannath MR. Sphingolipid Metabolic Pathway: An Overview of Major Roles Played in Human Diseases. Journal of Lipids. 2013;2013: 1-12.
8. Hanada K. Intracellular trafficking of ceramide by ceramide transfer protein. Proceedings of the Japan Academy, Series B. 2010;86: 426-437.
9. Funato K, Riezman H. Sphingolipid Trafficking. In: Hirabayashi Y, Igarashi Y, Merrill AH, editors. Sphingolipid Biology. Tokyo: Springer Japan, 2006:123-139.
10. Milhas D, Clarke CJ, Hannun YA. Sphingomyelin metabolism at the plasma membrane: Implications for bioactive sphingolipids. FEBS Letters. 2010;584: 1887-1894.
11. Hannun YA. THE SPHINGOMYELIN CYCLE AND THE 2ND MESSENGER FUNCTION OF CERAMIDE. JOURNAL OF BIOLOGICAL CHEMISTRY. 1994;269: 3125-3128.
12. Gutkind JS, Pirianov G, Vanek PG, et al. Suppression of ceramide-mediated programmed cell death by sphingosine-1-phosphate. Nature. 1996;381: 800-803.
13. Maceyka M, Spiegel S. Sphingolipid metabolites in inflammatory disease. Nature. 2014;510: 58.
14. Takabe K, Spiegel S. Export of sphingosine-1-phosphate and cancer progression. Journal of lipid research. 2014;55: 1839-1846.
15. Hong G, Baudhuin LM, Xu Y. Sphingosine-1-phosphate modulates growth and adhesion of ovarian cancer cells. FEBS Letters. 1999;460: 513-518.
16. Sutphen R, Xu Y, Wilbanks GD, et al. Lysophospholipids Are Potential Biomarkers of Ovarian Cancer. Cancer Epidemiology Biomarkers & Prevention. 2004;13: 1185.
17. Mikula-Pietrasik J, Uruski P, Szubert S, et al. Biochemical composition of malignant ascites determines high aggressiveness of undifferentiated ovarian tumors. Med Oncol. 2016;33: 94.
18. Xiao YJ, Schwartz B, Washington M, et al. Electrospray ionization mass spectrometry analysis of lysophospholipids in human ascitic fluids: comparison of the lysophospholipid contents in malignant vs nonmalignant ascitic fluids. Anal Biochem. 2001;290: 302-313.
19. Olivera A, Kohama T, Edsall L, et al. Sphingosine Kinase Expression Increases Intracellular Sphingosine-1-Phosphate and Promotes Cell Growth and Survival. The Journal of Cell Biology. 1999;147: 545-557.
20. Beach JA, Aspuria PJ, Cheon DJ, et al. Sphingosine kinase 1 is required for TGF-beta mediated fibroblast-to-myofibroblast differentiation in ovarian cancer, 2016.
21. Morad SAF, Cabot MC. Ceramide-orchestrated signalling in cancer cells. NATURE REVIEWS CANCER. 2013;13: 51-65.
22. Hannun YA, Luberto C, Mao C, Obeid LM, SpringerLink. Bioactive Sphingolipids in Cancer Biology and Therapy. Cham: Springer International Publishing, 2015.

23. Pyne NJ, Pyne S. Sphingosine 1-phosphate and cancer. NATURE REVIEWS CANCER. 2010;10: 489-503.
24. Creekmore AL, Silkworth WT, Cimini D, Jensen RV, Roberts PC, Schmelz EM. Changes in Gene Expression and Cellular Architecture in an Ovarian Cancer Progression Model. PLOS ONE. 2011;6: e17676.
25. Salmanzadeh A, Elvington ES, Roberts PC, Schmelz EM, Davalos RV. Sphingolipid Metabolites Modulate Dielectric Characteristics of Cells in a Mouse Ovarian Cancer Progression Model2013.
26. Ahmed N, Thompson EW, Quinn MA. Epithelial–mesenchymal interconversions in normal ovarian surface epithelium and ovarian carcinomas: An exception to the norm. Journal of Cellular Physiology. 2007;213: 581-588.
27. Liao JQ, Qian F, Tchabo N, et al. Ovarian Cancer Spheroid Cells with Stem Cell-Like Properties Contribute to Tumor Generation, Metastasis and Chemotherapy Resistance through Hypoxia-Resistant Metabolism. PLOS ONE. 2014;9: e84941.
28. McKeown SR. Defining normoxia, physoxia and hypoxia in tumours-implications for treatment response. BRITISH JOURNAL OF RADIOLOGY. 2014;87: 20130676.
29. Lippi G, Caleffi A, Pipitone S, et al. Assessment of neutrophil gelatinase-associated lipocalin and lactate dehydrogenase in peritoneal fluids for the screening of bacterial peritonitis. Clinica chimica acta; international journal of clinical chemistry. 2013;418: 59-62.
30. Burleson KM, Boente MP, Pambuccian SE, Skubitz APN. Disaggregation and invasion of ovarian carcinoma ascites spheroids. JOURNAL OF TRANSLATIONAL MEDICINE. 2006;4: 6-6.
31. Pattabiraman DR, Weinberg RA. Tackling the cancer stem cells - what challenges do they pose? NATURE REVIEWS DRUG DISCOVERY. 2014;13: 497-512.
32. Li HC, Fan XL, Houghton J. Tumor microenvironment: The role of the tumor stroma in cancer. JOURNAL OF CELLULAR BIOCHEMISTRY. 2007;101: 805-815.
33. Kalluri R, Zeisberg M. Fibroblasts in cancer. NATURE REVIEWS CANCER. 2006;6: 392-401.
34. Lu PF, Weaver VM, Werb Z. The extracellular matrix: A dynamic niche in cancer progression. JOURNAL OF CELL BIOLOGY. 2012;196: 395-406.
35. Thibault B, Castells M, Delord J-P, Couderc B. Ovarian cancer microenvironment: implications for cancer dissemination and chemoresistance acquisition. Cancer and Metastasis Reviews. 2014;33: 17-39.
36. Mitchell JB, McIntosh K, Zvonic S, et al. Immunophenotype of Human Adipose-Derived Cells: Temporal Changes in Stromal-Associated and Stem Cell–Associated Markers. STEM CELLS. 2006;24: 376-385.
37. Zuk PA, Zhu M, Ashjian P, et al. Human adipose tissue is a source of multipotent stem cells. Molecular biology of the cell. 2002;13: 4279-4295.
38. Shea AA. The Impact of Adipose-Associated Stromal Cells on the Metastatic Potential of Ovarian Cancer: Virginia Tech U6 - ctx_ver=Z39.88-2004&ctx_enc=info%3Aofi%2Fenc%3AUTF-8&rfr_id=info%3Asid%2Fsummon.serialssolutions.com&rft_val_fmt=info%3Aofi%2Ffmt%3Akev%3Amtx%3Abook&rft.genre=dissertation&rft.title=The+Impact+of+Adipose-Associated+Stromal+Cells+on+the+Metastatic+Potential+of+Ovarian+Cancer&rft.DBID=.9N&rft.au=Shea%2C+Amanda+Ann&rft.date=2014-01-22&rft.pub=Virginia+Tech&rft.advisor=Hulver%2C+Matthew+Wade&rft.externalDBID=com_10919_5534&rft.externalDocID=oai_vtechworks_lib_vt_edu_10919_54562&paramdict=en-US U7 - Dissertation, 2014.
39. Obesity and Cancer. Available from URL: https://www.cancer.gov/about-cancer/causes-prevention/risk/obesity/obesity-fact-sheet.
40. Delort L, Kwiatkowski F, Chalabi N, Satih S, Bignon Y-J, Bernard-Gallon DJ. Central Adiposity as a Major Risk Factor of Ovarian Cancer. Anticancer Research. 2009;29: 5229.
41. Nieman KM, Kenny HA, Penicka CV, et al. Adipocytes promote ovarian cancer metastasis and provide energy for rapid tumor growth. Nature medicine. 2011;17: 1498.

42. Kizaka-Kondoh S, Itasaka S, Zeng L, et al. Selective Killing of Hypoxia-Inducible Factor-1–Active Cells Improves Survival in a Mouse Model of Invasive and Metastatic Pancreatic Cancer. Clinical Cancer Research. 2009;15: 3433-3441.
43. Sphingosine-1-Phosphate Solubility Protocol & Cell Delivery. Available from URL: https://avantilipids.com/product/860492/.
44. Yu G, Wu X, Kilroy G, Halvorsen Y-DC, Gimble JM, Floyd ZE. Isolation of murine adipose-derived stem cells. Methods in molecular biology (Clifton, N.J.) U6 - ctx_ver=Z39.88-2004&ctx_enc=info%3Aofi%2Fenc%3AUTF-8&rfr_id=info%3Asid%2Fsummon.serialssolutions.com&rft_val_fmt=info%3Aofi%2Ffmt%3Akev%3Amtx%3Ajournal&rft.genre=article&rft.atitle=Isolation+of+murine+adipose-derived+stem+cells&rft.jtitle=Methods+in+molecular+biology+%28Clifton%2C+N.J.%29&rft.au=Yu%2C+Gang&rft.au=Wu%2C+Xiying&rft.au=Kilroy%2C+Gail&rft.au=Halvorsen%2C+Yuan-Di+C&rft.date=2011&rft.eissn=1940-6029&rft.volume=702&rft.spage=29&rft_id=info%3Apmid%2F21082392&rft.externalDocID=21082392&paramdict=en-US U7 - Journal Article. 2011;702: 29.
45. Sittampalam Gs CNPNHe, et al. Assay Guidance Manual. S.l. U6 - ctx_ver=Z39.88-2004&ctx_enc=info%3Aofi%2Fenc%3AUTF-8&rfr_id=info%3Asid%2Fsummon.serialssolutions.com&rft_val_fmt=info%3Aofi%2Ffmt%3Akev%3Amtx%3Abook&rft.genre=book&rft.title=Assay+Guidance+Manual&rft.au=Sittampalam+GS%2C+Coussens+NP%2C+Nelson+H%2C+et+al.%2C+editors&rft.date=2004-01-01&rft.pub=Eli+Lilly+%26+Company+and+the+National+Center+for+Advancing+Translational+Sciences&rft.externalDocID=ssib011432243&paramdict=en-US U7 - eBook: Eli Lilly & Company and the National Center for Advancing Translational Sciences, 2004.
46. Walzl A, Unger C, Kramer N, et al. The Resazurin Reduction Assay Can Distinguish Cytotoxic from Cytostatic Compounds in Spheroid Screening Assays. JOURNAL OF BIOMOLECULAR SCREENING. 2014;19: 1047-1059.